5-12-2023

Expanding the market of biomaterials

Franklin Quin Jr.
Mississippi State University, fquin2000@yahoo.com

Expanding the market of biomaterials

By

Franklin Quin, Jr.

Approved by:

Tamara Franca (Major Professor)
R. Dan Seale
Jason Tyler Street
Rubin Shmulsky (Graduate Coordinator)
L. Wes Burger (Dean, College of Forest Resources)

A Dissertation
Submitted to the Faculty of
Mississippi State University
in Partial Fulfillment of the Requirements
for the Degree of Doctor of Philosophy
in Sustainable Bioproducts
in the Department of Sustainable Bioproducts

Mississippi State, Mississippi

May 2023

Name: Franklin Quin, Jr.

Date of Degree: May 12, 2023

Institution: Mississippi State University

Major Field: Sustainable Bioproducts

Major Professor: Tamara Franca

Title of Study: Expanding the market of biomaterials

Pages in Study: 101

Candidate for Degree of Doctor of Philosophy

Biomaterials such as wood and bamboo are in high demand as a building material with the push for building with green technology. The wood product industry accounts for approximately 4% of the total U.S. manufacturing GDP (Gross Domestic Product), which is more than $100 billion. The industry supports over 752,000 full-time equivalent jobs, most of which are in rural areas where employment opportunities are limited. The estimated global market value of bamboo is estimated to be $60 billion annually. This research will explore the use of wood and bamboo in different end use products. The objectives of this research will 1) evaluate the behavior of two single bolt connections in the post-to-rail joint in a hardwood stairway system; 2) the potential of post-treating pre-fabricated cross-laminated timber (CLT) panels with two different copper based preservative treatments; and 3) estimated design values for a commercially sourced bolt laminated bamboo industrial mat. To accomplish these objectives, this dissertation is divided into five sections: 1) Introduction, 2) Structural performance of the post-to-rail connectors in a hardwood stairway handrail, 3) Development of preservative-treated cross-laminated timber: effects of panel layup and thickness on bonding

performance and durability when treated with copper-azole (CA-C) and micronized copper-azole (MCA), 4) Strength and stiffness of 3-ply industrial bamboo matting, 5) Conclusion.

DEDICATION

I would like to dedicate this work to my Lord and Savior Jesus Christ. For without Him I could do nothing, and to my beloved parents, Franklin Quin, Sr. and Esther B. Quin for instilling in me the value of education, and to my daughter, Celeiah Quin, for her love and encouragement during this journey.

ACKNOWLEDGEMENTS

I would like to express my appreciation and gratitude to my major supervisor, Dr. Tamara Franca, for her continuous support and supervision during this process. Thank you for your patience and understanding. I would like to thank Dr. R. Dan Seale, Dr. Jason T. Street, and Dr. Rubin Shmulsky for serving on my committee and providing input and guidance. I would like to thank Dr. Hyungsuk Lim for supporting and encouraging me to start on this journey. I would like to thank Dr. Jilei Zhang and Dr. Frank Owen for their support in getting me started on this journey and for their encouragement. I would like to thank Ms. Jeanie McNeel, Ms. Kay Davidson, Ms. Karen Williams, Ms. Marica McGinnis, Ms. Shawna Johnson, and Ms. Sharon Carr and the whole administrative staff for their support during this process. I would like my co-workers, Mr. David Butler, Mr. John Black, Dr. Edward Entsminger, Mr. Brain Mitchell, Mr. Chris McGinnis, and Mr. Demetrius Andol who was always willing to lend a hand when asked. I would like thank Samuel Ayanleye for his help with project planning and writing. I would like to take to whole Department of Sustainable Bioproducts for providing an environment conducive for learning. I would like to thank Shuqualak Lumber Company for providing the lumber. I would like to thank Fitts Industries, Inc. for providing the materials for the stair guard project. I would like to thank Henkel Company for donating the adhesive for this research. I would like to thank Deforest Wood Preserving and Koppers Performance Chemicals for treating our CLT panels.

TABLE OF CONTENTS

LIST OF TABLES

LIST OF FIGURES

CHAPTER I

INTRODUCTION

1.1 History of Wood as a Building Material

Wood has been considered a viable building material since the beginning of modern civilization (Perlin 1989). Wood is in high demand as a building material (Lattke and Lehmann 2007, Pajchrowski et al. 2014). Wood is an old construction material and it has been used worldwide to build shelter for thousands of years (Wimmers 2017). In the past, wood was used in the construction of large structures such as temples, towers, and bridges. However, use of wood for small residential buildings was not uncommon. Besides North America, most of the world substituted wood with bricks, steel and concrete for building. There are some factors impeding the use of wood in construction with the biggest being that wood is combustible (Koo 2013, Bartlett et al. 2019, Barber 2018). This issue was a large barrier driving builders to replace wood with non-combustible and non-flammable materials, which in some cases, these materials perform worse in fires when compared with wood. During the late 1990s and early 2000s, innovations in wood construction allowed wood to be used in the construction of large structures. Examples of these structures include the Stadthaus in London, UK (8 floors); the Forte in Melbourne, Australia (9 floors built with wood); the Wood Innovation and Design Center in Prince George, Canada (7 floors); the Treet in Bergen, Norway (14 floors); and, the Brock Commons in Vancouver, Canada (17 floors are built with wood). These building are not as tall as

steel or concrete buildings, but wood is indeed becoming competitor material for this type of construction (Pei et al. 2016, Wimmers 2017, Svatos-Raznjevic et al. 2022).

One of the main advantages that wood as a building material presents when compared to other building materials (concrete, steel, aluminum, or plastic), is that wood has lower embodied energy (Buchanan et al. 1999, Nassen et al. 2012). Embodied energy is the amount of energy required to harvest, mine, manufacture, and transport to the point of use of a material or product (Cabeza et al. 2013). Building with wood has environmental benefits (Falk 2009, FPL 2021). Wood is a renewable, sustainable, and eco-friendly material. In the United States, wood products represent approximately 80%-90% of residential construction (Conroy et al. 2018), but only about 10% market share in non-residential construction (Robichaud et al. 2009). Additionally, when wood is used in building construction, it helps in reducing greenhouse gas emissions and consequently helps in reducing global warming (Upton et al. 2008). Marsono (2015) stated that the building material has a big impact on the environment because of the potential to reduce a large portion of carbon dioxide emissions. Besides the environmental advantages that wood presents, historically wood has been chosen as the preferred material for construction because it is light-weight, versatile, and has desirable strength properties (Guestavsson and Sathre 2006, Ngohe-Ekram et al. 2006, Profft et al. 2009, Tsunetsugu and Tonosaki 2010, Agoudjil et al. 2011, Ingerson 2011).

However, as previously stated, most of the residential construction has been in low-rise construction and the advancement of wood as a building material has relatively been related to the public's perception of wood as a building material (Kozak and Cohen 1997, O'Connor et al. 2004). Therefore, knowledge in wood science and technology is important to enhance the competitiveness of wood products with other products such as concrete and steel, and

consequently promoting better utilization of natural resources, and contributing to the economic development of local communities and environmental health. Ramage et al. (2017) stated that the highest value products that comes from trees is structural-graded lumber and engineered wood products.

1.2 Differences and uses of hardwoods and softwoods

Wood products are divided into two broad classes, referred to as hardwoods and softwoods, and this will depend on the type of tree they came from. Hardwoods or also known as angiosperms have enclosed seeds in the ovary of the flower. On the other hand, softwoods, or gymnosperms have seeds not enclosed in the ovary of the flower (Barker and Owen 1999).

The anatomical features of softwoods and hardwoods also differ, and these distinguished features directly affect the performance of wood products. They present different cell types and arrangements, whereas hardwoods have a complex anatomical structure compared to softwoods (Barnett and Jeronimidis 2003). The main difference between hardwood and softwood is the absence of porous/vessel cells in softwood anatomical structure. Vessels are responsible for transporting water or sap in the tree. Softwoods are nonporous and are mainly composed of elongated cells called tracheids that are responsible for water transport and mechanical strength (Brown et al. 1949).

Gaston (2014) states that most softwoods in North American are consumed in new residential construction, residential repair and renovation. Softwoods are used in construction for forms, scaffolding, framing, sheathing, flooring, molding, paneling, cabinets, poles, piles, and many other building components. Hardwoods are used in construction for flooring, architectural woodwork, interior woodwork, paneling, and stair guard systems (Wiemann 2021).

1.3 Overview of physical and mechanical properties of wood

Wood quality is dependent upon it physical and mechanical properties. Since wood is a biological material, its properties are influenced by a vast array of environmental conditions. The definition of wood quality varies depending upon the intended end use (MacDonald and Hubert 2002). The quality of wood depends on its physical properties such as specific gravity (SG) or density, moisture content (MC), percentage of latewood, and number of rings per inch (RPI); mechanical properties such as bending stiffness (modulus of elasticity[MOE]), bending strength (modulus of rupture[MOR]), compression strength, tensile strength, hardness, and shear strength; and anatomical properties such as microfibril angle and cell wall thickness (Megraw 1985; Briggs 2010). Wood quality highly depends on SG because of its high correlation with wood strength. Because wood is hygroscopic meaning it takes on moisture from the surrounding environment, the physical and mechanical properties are also dependent upon the wood moisture content. The exchange of moisture between wood and air depends on the amount of moisture in the air (relative humidity), air temperature, and the moisture content of the wood, and as the moisture content of wood changes, the wood could experience shrinkage and swelling which could lead to wood degrade (Panshin and Zeeuw 1964).

Wood is also an orthotropic material; its' mechanical properties are dependent upon the directions of three mutually perpendicular axes: longitudinal, radial, and tangential. The longitudinal axis parallel to the grain direction while the radial axis and the tangential axis are perpendicular to the grain direction. The radial axis is also normal to the growth rings, while the tangential axis is tangent to the growth rings (Senalik and Farber 2021).

1.4 Stair guard systems (post-to-rail connection)

The use of wood especially hardwoods such as red oak (*Quercus rubra*), white oak (*Quercus alba*), yellow poplar (*Liriodendron tulipifera*), and hard maple (*Acer saccharum*), has been the main construction material for stair cases over the years. Staircase designs has evolved because of the flexibility of wood and working with specialized manufacturing machinery. On the job site, stair builders prefer wood because of its appearance, ease of workability, and it can be shaped and fabricated with inexpensive tools (Cooper 2014). Wood allows staircase designs to be easily fabricated according to a consumer's needs.

One of the important components of the stair guard system is the handrail. The handrail consists of the handrail component along with the connections linking the handrail to the stair guard system. The stair guard system can be broken down into five connections: post-to-footing; post-to-rail; infill(baluster)-to-footing; infill(baluster)-to-rail; and rail-to-rail (Wynne et al. 2000). A stair guard system connection must be designed to resist rotational and translational movements whenever a force is applied to the handrail.

The Stairbuilders and Manufacturers Association (SMA), established in 1988 to ensure the growth and sustainability of the stair case industry, publishes guidelines for the installation of a residential stairway system and these guidelines are based upon the experience of the stair builder's knowledge gained over the years. SMA works to promote stairway safety through scientific research and testing (Cooper 2014). For wood to remain competitive against alternative materials in staircase construction, design values for wood and the connections need to be developed through research and testing.

In the building code (ASCE/SEI 7-10 – Minimum Design Loads for Buildings and Other Structures) published by the American Society of Civil Engineers (ASCE), the handrail and

guardrail systems should be designed to “resist a single concentrated load of 200 lb applied in any direction at any point along the top and to transfer this load through the supports of the structure” (ASCE 2005). In a stair guard system, the connections used to connect the components are important. Loferski et al. (2006) investigated posts connections in residential decks under monotonic loading. The study focused on determining if the connection system could pass the ASCE/SEI 7-10 code requirement of the 200 lb concentrated load. The authors tested four No. 2 southern yellow pine connection systems only two successfully passed the code requirements.

Pousette (2006) and Pencik (2015) studied the connection between the tread and string in a wooden stair system. This study was built upon collecting experimental data in order to validate finite element (FE) models of the connection. Other studies have evaluated and showed the potential of using hardwood species for structural purposes (Bendtsen et al. 1975 and Koch 1985). Adhikari et al. (2021) emphasized there is a high demand for hardwood products and there is a need for a deeper understanding on the mechanical behavior of hardwood species.

1.5 Southern yellow pine lumber and its importance to the market

Structural lumber is mainly cut from softwood trees because of its versatility and strength, in addition to fast growth rate, the harvest time is faster than hardwoods. In most cases softwoods cost less to harvest than hardwoods (Krackler et al. 2011).

A large market share of wood in the construction industry in the United States belongs to southern pine lumber (Gaby 1985) and the demands for lumber and timber products has steadily increased over the past decades because of the increase in world population and disposable income (Oswalt et al. 2009). Southern yellow pine (SYP) grows throughout the southern part of the United States and this species group is made up of primarily four trees: loblolly pine (*Pinus*

taeda), longleaf pine (*Pinus palustris*), shortleaf pine (*Pinus echinate*), and slash pine (*Pinus eliottii*), where the largest percentage of the species group belong to loblolly pine (Franca 2021).

Southern pine lumber is known for its strength, stiffness, ease of treatability with preservatives, tool workability, and drying efficiency. The southern region of the US is home to large scale timber and lumber manufacturing. It is estimated that around 60% of the lumber used in the United States and 15% of the lumber consumed globally comes from the southern region of the United States (Wear and Greis 2002; McKeand et al. 2003). This in turn makes this region important to the economics of the United States. SYP lumber accounts for about 50% of the softwood lumber produced in the United States (US Census Bureau 2011).

In order to maintain lumber quality consistency in the lumber market, lumber is sold based upon a grading system. Grading is necessary to minimize differences between materials because of within species variation. SYP lumber is graded according to rules set forth by the Southern Pine Inspection Bureau (SPIB) which is approved by the American Lumber Standard Committee (ALSC) and this grading system allows the lumber to be classified based upon certain grading criteria.

Lumber can be visually graded, or machine graded or a combination of both. Visually graded lumber is based upon grading rules established from the testing of clear wood samples along with estimated strength reducing and grading reducing defects (Monetero et al. 2011). Machine graded lumber is based upon visual evaluation along with some form of nondestructive evaluation for estimating lumber strength. Lumber produced through machine grading has a lower coefficient of variation than lumber produced through visual grading (Brown et al. 1997, Winistorfer and Theilen 1997).

1.6 Mass timber and cross-laminated timber products

The global construction industry according to the International Energy Agency in 2018 accounted for 11% of total energy and process related CO_2 emissions into the environment (Lan 2020). This number is expected to increase as the global population continues to rise and the demand for affordable housing. Historically, timber products have mainly been used on light-frame, single-story buildings. However, a new group of wood products called mass timber (MT) fabricated from either dimension lumber, veneers or strands have permitted wood to compete in the mid-rise, and high-rise buildings market. Examples of MT include cross-laminated timber (CLT), dowel-laminated timber (DLT), glue-laminated timber (Glulam), nail-laminated timber (NLT), laminated strand lumber (LSL), laminated veneer lumber (LVL), parallel strand lumber (PSL), and mass plywood panel (MPP). MT-based building has become increasingly popular due to its sustainability. MT has been fabricated to be used in roof construction, columns, walls, and floors in mid-rise to high-rise building construction as an alternative to concrete and steel (Anderson et al. 2020, D'Amico et al. 2021).

One of the most recent innovations in wood and building industry is CLT, an engineered wood product (EWP) manufactured from dimensions lumber stacked in layers at 90° to the previous layer. CLT panels usually can be manufactured from 3-layers up to 9-layers. CLT was first developed in European countries in the 1970s and 1980s and has enjoyed a major level of success in the European construction market and is establishing a presence in North American construction projects (Brandner et al. 2016).

CLT is an innovative product that not only has a high strength-to-weight ratio, but also has a low carbon footprint and is a sustainable alternative to steel and concrete (Hammond and Jones 2008, Pierobon et al. 2019). The demand for the use of CLT has been steadily increasing

over the past decade in North American (Muszynski et al. 2017). A CLT building behaves as a 'carbon sink' it allows large quantities of carbon to be stored over a long time period (Lehmann 2012). Other advantages of CLT is dimensional stability (cross-lamination), flexibility in design (accurate prefabrication cuts of the panels and openings), and fast on-site installation. CLT has shown to have good thermal and acoustic performance. There are approximately 816 structural grade CLT projects in the US that are either built, being built, or in the design stages (Woodworks 2022).

With the introduction of CLT the use of timber products in multi-story buildings have become a reality. The specifications for the manufacturing of CLT in the United States and Canada are published in ANSI/APA PRG 320 (ANSI/APA 2019). The CLT standard PRG 320 is recognized by the American National Standards Institute (ANSI). The National Design Specification (NDS) for wood construction incorporates CLT as a viable building material. This specification was referenced in the 2015 International Building Code (IBC), which means that CLT is a code-compliant construction material (International Code Council 2015). Most structural grade CLT is manufactured using softwoods as specified in the CLT standards handbook (ANSI/APA 2019), with a growing interest in utilizing hardwoods in the manufacturing of CLT (Espinoza 2018). Some hardwoods are naturally more durable than other hardwoods. CLT can be used for floors, roofs, exterior walls, and partition walls.

1.7 Bamboo, a wood alternative

As the push for building green continues, the demand for wood for construction use will continue to increase. To help with the increase demand for wood an alternative to constructing with wood could be bamboo. Bamboo is classified as one of the fastest-growing and strongest plants in the world. Bamboo forests are spread widely across regions of Asia, Africa, and Latin

America (Hu 2022). There are many bamboo species in the world, but there are only two native bamboo species in the United States. There has been a number of bamboo species imported into the United States and planted in the southeastern states and California. One such species of bamboo that has been grown in South Carolina for over 70 years is giant timber bamboo (*Phyllostachys bambuisoides*) (Lee 1994). The International Network of Bamboo and Rattan (INBAR) estimated the total global bamboo forests in 2020 was more than 35 million hectares. Bamboo has a rapid grown/harvest cycle as compared to trees. Bamboo can be harvested in 5 years, whereas some softwoods such as the southern pines are usually harvested in 25 years. Engineered wood panels can be produced from bamboo such as laminated bamboo lumber (LBL), bamboo-oriented strand board (OSB), and scrimber (a high strength product that is formed by changing the cell structure of bamboo through high pressure and adhesives). Products made from bamboo can be manufactured to high strength and stiffness in order to be used for sustainable construction (Xiao 2010). The tensile strength of a bamboo fiber (650 MPa) is twice that of wood and close that of steel (500 to 1,000 MPa) (Qiu 2019).

1.8 Objectives

Expanding the market potential of biomaterials (wood and bamboo) as a building material was explored in this study. Wood and bamboo have proven to be a viable and sustainable resource that influences the environment and the economics of a community. By increasing the knowledge base of how wood and bamboo can be used in various applications is very beneficial.

This research evaluated three aspects of expanding the use of biomaterials as a building material: 1) determine the structural performance of the connectors in a hardwood stairway handrail guard components for the post-to-rail connection, 2) evaluation of the panel bond

quality and durability of post-treated SYP CLT panels treated with a copper azole (CA-C) and micronized copper azole (MCA) treated to AWPA UC4A (ground contact or fresh water specifications), and 3) evaluation of the strength and stiffness of a commercially sourced industrial bamboo mat.

1.9 References

Adhikari S, Quesda H, Bond B, and Hammett T. 2021. Current Status of the US Hardwood Sawmills to Produce Structural Grade Hardwood Lumber. Mass Timber Construction Journal 4(1):10-18.

Agoudjil B, Benchabane A, Boudenne A, Ibos L, and Fois M. 2011. Renewable Materials to Reduce Building Heat Loss: Characterization of Date Palm Wood. Energy Build 43:491-497.

American Society of Civil Engineers (ASCE). 2005. ASCE 7-05/ANSI A58. Minimum Design Loads for Buildings and Other Structures. ASCE. Reston, VA.

Anderson R, Atkins D, Beck B, Dawson E, and Gale CB. 2020. State of the Industry: North American Mass Timber 156p.

APA- The Engineered Wood Association. 2018. PRG 320-2019. Standard for Performance-Rated Cross-Laminated Timber. Tacoma, WA.

Barber D. 2018. Fire Safety of Mass Timber Buildings with CLT in USA. Wood and Fiber Science 50:83-95.

Barker B and Owen N. 1999. Identifying Softwoods and Hardwoods by Infrared Spectroscopy. Journal of Chemical Education 76(12):1706-1709.

Barnett JR and Jeronimidis G. 2003. Wood Quality and its Biological Basis. CRC Press.

Bartlett A, Hadden R, and Bisby L. 2019. A Review of Factors Affecting the Burning Behaviour of Wood for Application to Tall Timber Construction. Fire Technology 55:1-49.

Bendtsen B and Ethington R. 1975. Mechanical Properties of 23 Species of Eastern Hardwoods. USDA Forest Service. Forest Products Laboratory. Report No. 230. Madison, WI. 12p.

Brandeis C, Taylor M, Abt K, Alderman D, and Buehlmann U. 2021. Status and Trends for the U.S. Forest Products Sector. USDA Forest Service. Southern Research Station. GTR-SRS-258. Asheville, NC. 55 pp.

Brandner R, Flatshcer G, Ringhofer A, Schickhofer G, and Thiel A. 2016. Cross laminated Timber (CLT): Overview and Development. European Journal of Wood and Wood Products 74:331-351.

Briggs D. 2010. Enhancing Forest Value Productivity Through Fiber Quality. Journal of Forestry. 108(4):174-182.

Brown HP, Panshin AJ, and Forsaith CC. 1949. Texbook of Wood Technology, McGraw-Hill Book Company Inc. New York, NY.

Brown LS, De Visser DA, Tuvey RS, and Rozek AK. 1997. Mechanically Graded Lumber: A Grading Agency Perspective. Wood Design Focus 8(2):3-7.

Buchanan AH and Levine SB. 1999. Wood-Based Building Materials and Atmospheric Carbon Emissions. Environmental Science and Policy 2:427-437.

Cabeza L, Barreneche C, Miró L, Morera J, Bartolí E, and Fernández A. 2013. Low Carbon and Low Embodied Energy Materials in Buildings: A Review. Renewable and Sustainable Energy Reviews 23:536-542.

Conroy K, Riggio M, and Knowles C. 2018. Familiarity, Use, and Perceptions of Wood Building Products: A Survey Among Architects on the United States West Cost. Bioproducts Business 3(10):118-135.

Cooper DSM and River F. 2014. The Demand for Structural Appearance-Grade Hardwoods. National Hardwood Magazine 4:44-45.

Dahlen J, Jones PD, Seale RS, and Shmulsky R. 2014. Bending Strength and Stiffness of Wide Dimension Southern Pine No. 2 Lumber. European Journal of Wood and Wood Products 72:759-768

D'Amico B, Pomponi F, and Hart J. 2021. Global Potential for Material Substitution in Building Construction: The Case of Cross Laminated Timber. Journal of Cleaner Production 279(1):123487.

Ellis R. 1940. Knots and the Desirability of Pruning. BS thesis. Oregon State College, Corvallis, Oregon. 35 pp.

Espinoza O and Buehlmann U. 2018. Cross-Laminated Timber in the USA: Opportunity for Hardwoods. Current Forestry Reports 4:1-12.

Falk B. 2009. Wood as a Sustainable Building Material. Forest Products Journal 59(9):6-12.

FPL. 2021. Wood handbook – Wood as Engineering Material. USDA Forest Service, Forest Products Laboratory, Madison, WI, FPL-GTR-282. 543 pp.

Franca FJN, Shmulsky R, Ratcliff JT, Farber B, Senalik CA, Ross RJ, and Seale RD. 2021. Yellow Pine Small Clear Flexural Properties Across Five Decades. Forest Products Journal 71(3):233-239.

Gaby L. 1985. Southern Pines: Loblolly Pine (*Pinus taeda* L.), Longleaf Pine (*Pinus palustris* Mill.), Shortleaf Pine (*Pinus echinate* Mill.), Slash Pine (*Pinus elliottii* Engelm.). USDA Forest Service. Forest Products Laboratory. FS-256 Madison, WI. 10 pp.

Gagnon S and Pirvu C. 2011. CLT Handbook-Canadian Edition. FP Innovations.

Gaston C. 2014. Visual Wood Product Trends in North American Nonresidential Buildings. Forest Products Journal 64(3-4):107-115.

Gustavsson L and Sathre R. 2006. Variability in Energy and Carbon Dioxide Balances of Wood and Concrete Buildings Materials. Building and Environment 41(7):940-951.

Hammond GP and Jones CI. 2008. Embodied Energy and Carbon in Construction Materials. Proceedings of the Institution of Civil Engineers 161(2):87-98.

Hu Y, Xiong L, Li Y, Semple K, Nasir V, Pineda H, He M, and Dai C. 2022. Manufacturing and Characterization of Wide-Bundle Bamboo Scrimber: A Comparison with Other Engineered Bamboo Composites. Materials 15:7518.

Ingerson A. 2011. Carbon Storage Potential of Harvested Wood: Summary and Policy Implications. Mitigation and Adaptation Strategies for Global Change 16:307-323.

Koch P. 1985. Utilization of Hardwood Growing on Southern Pine Sites - Volume 1. Agriculture Handbook SFES-AH-605. Asheville, NC: USDA-Forest Service, Southern Forest Experiment Station. 1-1418.

Koo K. 2013. A Study on Historical Tall-Wood Buildings in Toronto and Vancouver. FPInnovations, Pointe-Claire, Que., Canada.

Kozak RA and Cohen DH. 1997. How Specifiers Learn About Structural Materials. Wood and Fiber Science 29(4):381-396.

Krackler V, Keunecke D, Niemz P, and Hurst A. 2011. Possible Fields of Hardwood Application. Wood Research 56(1):125-136.

Lan K, Kelley S, Nepal P, and Yao Y. 2020. Dynamic Life Cycle Carbon and Energy Analysis for Cross-Laminated Timber in the Southeastern United States. Environmental Research Letters 15:12.

Lattke F and Lehmann, S. 2007. Multi-Storey Residential Timber Construction: Current Developments in Europe. Journal of Green Building 2(1):119-129.

Lehmann S. 2012. Sustainable Construction for Urban Infill Development Using Engineered Massive Wood Panel Systems. Sustainability 4(10):2707-2742.

Lee AWC, Bai X, and Peralta P. 1994. Selected Physical and Mechanical Properties of Giant Timber Bamboo Grown in South Carolina. Forest Products Journal 44(9):40-46.

Loferski JR, Albright D, and Woeste PE. 2006. Tested Guardrail Post Connections for Residential Decks. Wood Design Focus 16(2):13-18.

Lowell E, Maguire D, Briggs D, Turnblom E, Jayawickrama K, and Bryce J. 2014. Effects of Silviculture and Genetics on Branch/Knot Attributes of Coastal Pacific Northwest Douglas-Fir and Implications for Wood Quality–A Synthesis. Forests 5:1717-1736.

Macdonald E and Hubert J. 2002. A Review of the Effects of Silviculture on Timber Quality of Sitka Spruce. Forestry 75(2):107-138.

Marsono A and Balasbaneh A. 2015. Combinations of Building Construction Material for Residential Building for the Global Warming Mitigation for Malaysia. Construction and Building Materials 85(6):100-108.

McKeand S, Mullin T, Byram T, and White T. 2003. Deployment of Genetically Improved Loblolly and Slash Pine in the South. Journal of Forestry 100(3):32-37.

Megraw RA. 1985. Wood Quality Factors in Loblolly Pine: The Influence of Tree Age, Position in Tree, and Cultural Practice on Wood Specific Gravity, Fiber Length and Fibril Angle. TAPPI Press, Atlanta, GA. 88 p.

Montero M, Mateo R, Iniguez-Gonzalez G, Martitegui F, Hermoso E, and Esteban M. 2011. Visual Grading of Large Cross Section Structural Timber of *Pinus sylvestris* L. According to UNE 56544: 2007 standard. Pages 1-6. In SHATIS'11 International Conference on Structural Health Assessment of Timber Structures. Libson, Portugal.

Muszynski L, Hansen E, Fernando S, Schwarzmann G, and Rainer J. 2017. Insights into the Global Cross-Laminated Timber Industry. BioProducts Business 2(8):77-92.

Nassen J, Hedenus F, Karlsson S, and Holmberg J. 2012. Concrete vs. Wood in Buildings - An Energy System Approach. Building and Environment 51(5):361-369.

Ngohe-Ekam PS, Meukam P, Menguy G, and Girard P. 2006. Thermophysical Characterization of Tropical Wood used as Building Materials: With Respect to the Basal Density. Construction and Building Materials 20:929-938.

O'Connor J, Kozak R, Gaston C, and Fell D. 2004. Wood use in Non-Residential Buildings: Opportunities and Barriers. Forest Products Journal 54(3):19-28.

Oswalt SN, Thompson M, and Smith WB. 2009. US Forest Resource Facts and Historical Trends. FS-801. USDA, Forest Service.

Pajchrowski G, Noskowiak A, Lewandowska A, and Strykowski W. 2014. Wood as a Building Material in the Light of Environmental Assessment of Full Life Cycle of Four Buildings. Construction and Building Materials 52(2):428-436.

Panshin AJ and Zeeuw CD. 1964. Texbook of Wood Technology, McGraw-Hill Book Company Inc., New York, NY.

Pei S, Rammer D, Popovski M, Williamson T, Line P, and van de Lindt JW. 2016. An Overview of CLT Research and Implementation in North America. In: World Conference on Timber Engineer, WCTE 2016. 22-25 August 2016; Vienna, Austria. 10pp.

Pencik J. 2015. Analysis of Support of Stairs in a Wooden Prefabricated Staircase with One-sided Suspended Stairs Made from Scots Pine (*Pinus Sylvestris*) with the Use of Experimental Tests and Numerical Analysis. Wood Research 60(3):477-490.

Perlin J. 1989. A Forest Journey. The Role of Wood in the Development of Civilization. Harvard University Press, Cambridge. Originally published by W.W. Norton, New York. 445pp.

Pierobon F, Huang M, Simonen K, and Ganguly I. 2019. Environmental Benefits of Using Hybrid CLT Structure in Midrise Non-Residential Construction: An LCA Based Comparative Case Study in the U.S. Pacific Northwest. Journal of Building Engineering 26(11):1-14.

Pousette A. 2006. Testing and Modeling of the Behavior of Wooden Stairs and Stair Joints. Journal of Wood Science 52:358-362.

Profft I, Mund M, Weber GE, Weller E, and Schulze ED. 2009. Forest Management and Carbon Sequestration in Wood Products. European Journal of Forest Research 128:399-413.

Qiu H, Xu J, He Z, Long L, and Yue X. 2019. Bamboo as an Emerging Source of Raw Material for Household and Building Products. BioResources 14(2):2465-2467,

Ramage M, Burridge H, Busse-Wicher M, Fereday G, Reynolds T, Shah D, Wu G, Yu L, Fleming P, Densley-Tingley D, Allwood J, Dupree P, Linden PF, and Scherman O. 2017. The Wood from the Trees: The Use of Timber in Construction. Renewable and Sustainable Energy Reviews 68:333-359.

Robichaud F, Kozak R, and Richelieu A. 2009. Wood Use in Non-Residential Construction: A Case for Communication with Architects. Forest Products Journal 59(1/2):57-65.

Senalik CA and Farber B. 2021. Mechanical Properties of Wood. Pages 5.1-5.46, Wood Handbook. USDA Forest Service. Forest Products Laboratory. FPL-GTR-190. Madison, WI.

Svatos-Raznjevic H, Orozco L, and Menges A. 2022. Advanced Timber Construction Industry: A Review of 350 Multi-Story Timber Projects from 2000-2021. Buildings 12(404):1-42.

Tsunetsugu Y and Tonosaki M. 2010. Quantitative Estimation of Carbon Removal Effects due to Wood Utilization up to 2050 in Japan: Effects from Carbon Storage and Substitution of Fossil Fuels by Harvested Wood Products. Journal of Wood Science 56:339-344.

Upton B, Miner R, Spinney M, and Heath L. 2008. The Greenhouse Gas and Energy Impacts of Using Wood Instead of Alternatives in Residential Construction in the United States. Biomass and Bioenergy 32(1):1-10.

US Census Bureau. 2011. Lumber Production and Mill Stocks-2010.

Wang J, Wei P, Gao Z., and Dai C. 2018. The Evaluation of Panel Bond Quality and Durability of Hem-Fir Cross-Laminated Timber (CLT). European Journal of Wood and Wood Products 76:833-841.

Wear DN and Greis JS. 2002. Southern Forest Resource Assessment: Summary of Findings. Journal of Forestry 100(7):6-14.

Wiemann MC. 2021. Characteristics and Availability of Commercially Important Woods. Pages 2.1-2.45, Wood Handbook: USDA Forest Service. Forest Products Laboratory: FPL-GTR-190. Madison, WI.

Wimmers G. 2017. Wood: A Construction Material for Tall Buildings. Nature Reviews Materials 2(17051).

Winistorfer SG and Theilen RD. 1997. Machine-Graded Lumber-Design Implications. Wood Design Focus 4(3):3-7.

WoodWorks. 2022. Building Trends: Mass Timber: Quarterly Update + Map of U.S. Mass Timber Projects. Woodworks.org.

Wynne D, Hampton S, Cregger N, and Suits C. 2000. A Comprehensive Visual Guide of Stair Parts and Stair Construction. Coffman Stair Building Guide, Coffman Stairs LLC, Marion, Virginia.

CHAPTER II

STRUCTURAL PERFORMANCE OF THE POST-TO-RAIL CONNECTORS IN A HARDWOOD STAIRWAY HANDRAIL GUARD

2.1 Abstract

The performance of two single bolt post-to-rail connection systems for a stairway handrail was evaluated. These two connection systems are popular in the stairway construction industry because of the ease of use. Red oak posts and rails along with the connection hardware was secured from a local stairway hardwood supply manufacturer. T-shaped cantilever typed joints were constructed to determine the initial stiffness, yield rotation, yield strength, ductility, and strength at a rotation of 0.15 radians under monotonic and reverse-cyclic loading. There was a difference between the initial stiffness of the joint configurations, but there was no significant difference between the yield strength and the maximum strength. Both joint configurations proved to be ductile with the major modes of failure being compression of the wood on the rail and post and the yielding of the bolt in bending.

2.2 Introduction

Stairs are a part of our everyday life and can present a serious safety hazard if not designed properly. Some of the major factors that influence stairway safety is variability in rise and run, stair steepness, and handrail design (Templer et al. 1985). The purpose of the handrail is to aid in preventing falls and the severity of falls on the staircase. Maki (1985) conducted a study that showed the normal forces and moments that individuals exerted on the handrail by standing

in an upright position holding onto the handrail. These forces would be more severe when preventing a fall.

Most hardwood stairway guard components are manufactured according to traditional design with dimensions and mechanical properties based on the experience of the stair builder. Stairways are often designed from an aesthetic point of view as compared to an engineering design view. The mechanical behavior of a stairway system is usually modeled using simple beam calculations with special computer programs (Pousette 2006).

The mechanical properties of the materials as well as the joints are important factors to determine the structural behavior of the stairway system. The connection between the post and handrail are usually made with different types of connectors and are usually not glued. There are certain variables that can be changed in this type of joint such as the thickness of the rail, the size of the hole drilled in the rail or post, the dimensions of the fasteners, stiffness of the connection, and actual properties of the wood (Pousette 2006 and Pencik 2015).

The literature states that a beam is a tri-dimensional member with one dimension significantly greater than the other two. Based upon that assumption the Euler-Bernoulli simple beam theory can be used to analyze the data (Bauchau and Craig 2009).

This study assumed that the handrail was considered to behave as a cantilever beam loaded at one end and fixed at the other end. The purpose of this study was to evaluate the structural performance of two different types of concealed single-bolt connectors linking the post-to-handrail of a stairway guard system. Two common post-to-rail connectors used by the stairway builder's industry were used in this study.

2.3 Materials and Methods

2.3.1 Wood Species

Kiln-dried, defect-free, and straight-grained glue laminated red oak (*Quercus rubra*) rails (2 ½" x 1 ¾" x 45") and posts (3 ½" x 3 ½" x 44") used by staircase manufacturers were secured from Fitts Industries, Inc. in Tuscaloosa, AL. The average moisture content of the red oak specimens was 7.4% as measured following ASTM D 4442 (ASTM 2020). The rails and posts were cut to size in the wood shop at the Department of Sustainable Bioproducts at Mississippi State University, Starkville, MS. The posts and rails were kept in a controlled environment (21 °C and 65% relative humidity (RH)) for several weeks until joint fabrication. Each joint specimen was identified by configuration number (C1 and C2), type of load applied (S for static, M for monotonic, and C for reversed cyclic), and repetition number (1 to 5). For example, the third repetition, under monotonic load, for configuration #2 had the label C2-M-3.

2.3.2 Rail & Post Fastener #301 (Configuration 1) (C1)

The rail & post fastener #301 (Figure 2.1) is widely used in the staircase industry to link posts to treads and/or rails. This connector also is typically used were a normal rail-bolt connector #302 will not work. For the rail & post fastener #301, a 1" x 2 ½" deep hole was drilled in the center of the wide face of the post. A 7/16" hole was then drilled through the 1" hole in the post to the outside of the post. A ¼" x 2" deep hole was drilled into the center cross section of the rail. The 3/8" lag screw was then inserted through the 7/16" hole in the post and then screwed into the ¼" hole in the rail with a socket wrench until the post was snug against the rail. Figure 2.2 shows the rail & post fastener #301 configuration.

Figure 2.1 Rail & Post Fastener #301 (3/8” lag screw, 7 threads/inch)

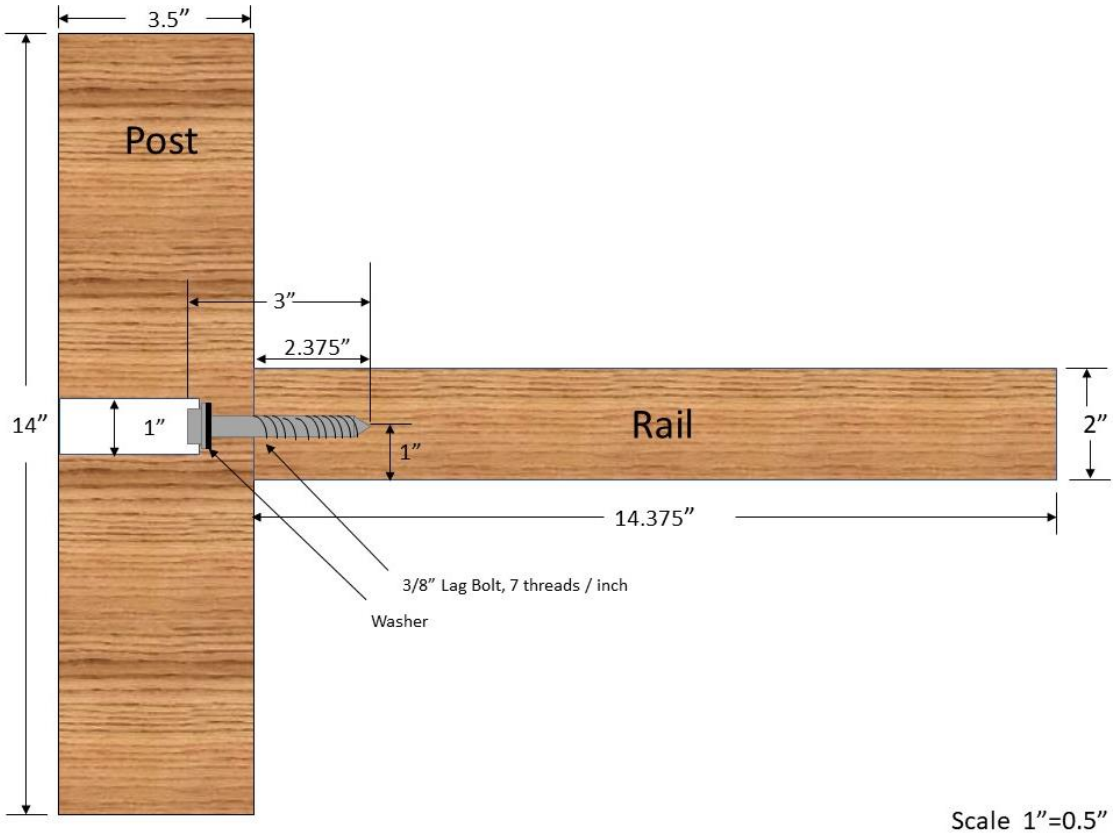

Figure 2.2 Rail & Post Fastener #301 Joint

2.3.3 Rail-Bolt Fastener #302 (Configuration 2) (C2)

The rail-bolt fastener #302 (Figure 2.3) is commonly used to secure rails to posts. For the rail-bolt fastener #302, a ¼” x 2” deep hole was drilled into the center of the wide face of the post. The lag-screw thread end of the hanger bolt was inserted into the post with a rail-bolt wrench. A 3/8” x 2” deep hole was drilled in the center cross section of the rail, and a 1” hole was drilled 1 ½” from the end of the rail to a depth of 1 ½”. A plastic washer was then inserted into the 1” hole in the rail. The rail was then inserted onto the machine-bolt thread end of the hanger bolt on the post through the 3/8” hole in the rail and through the plastic washer. A serrated flange metal nut was then inserted into the 1” hole in the rail and fastened to the

machine end of the rail-bolt using the rail bolt wrench. Figure 2.4 shows the rail-bolt fastener #302 configuration.

Figure 2.3 Rail-Bolt Fastener #302 (5/16-18 hanger bolt)

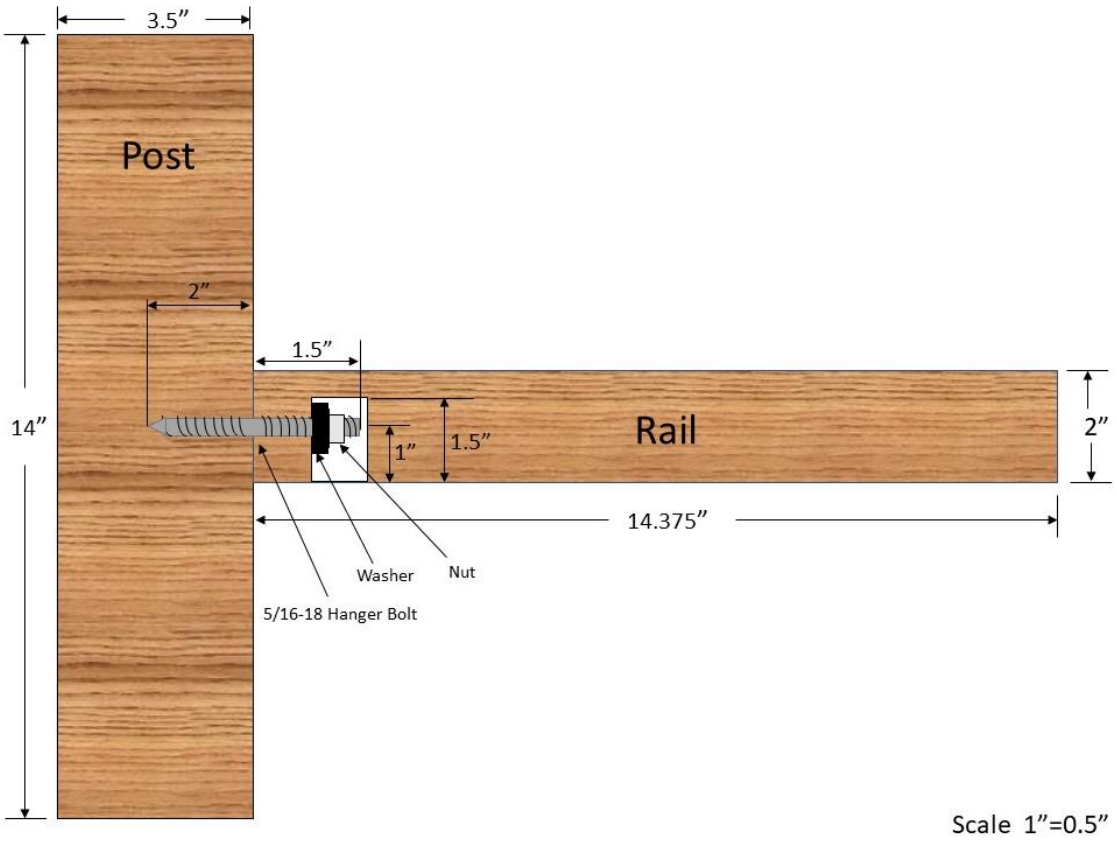

Figure 2.4 Rail-bolt fastener #302 joint

2.3.4 Loading Protocol and Measurements

2.3.4.1 Static Loading

The maximum moment carry capacity of the post-to-rail joints were evaluated by cantilever bending tests. Ten joints (C1-S-1, C1-S-2, C1-S-3, C1-S-4, C1-S-5, C2-S-1, C2-S-2, C2-S-3, C2-S-4, C2-S-5) were tested. The bending moment arm was 12”. Two linear variable differential transformers (LVDTs) were installed parallel to the rail for measuring the rail’s rotational movement. The two parallel LVDTs were placed on top and bottom 3 ½” away from the post, on rail’s center. The distance between the LVDTs was 3 3/8”. One wire LVDT located on the neutral axis of the rail 10” from the post was used to measure the rail displacement at 10” from the post. The joint rotation was measured in radians with equation 2.1:

$$\theta\ (rad) = \arctan\left((yt + yb)/d\right) \tag{2.1}$$

where θ is joint rotation in radians, yt is movement of top LVDT, yb is movement of bottom LVDT, and d is distance between LVDTs (3 3/8”), respectively. The LVDTs were positioned 3 ¼” from the post on the top and bottom sides of the rail.

The joints were tested until failure on a SATEC (Intron) Universal Testing Machine Model 8800 at a loading rate of 0.5 in/min. The load was applied perpendicular to the rail top, while the test specimen was horizontally placed on the machine testing bed. The post was secured to the machine testing bed with two 18” x 3.75” x 0.75” A36 steel plates and four 0.5” x 24” bolts.

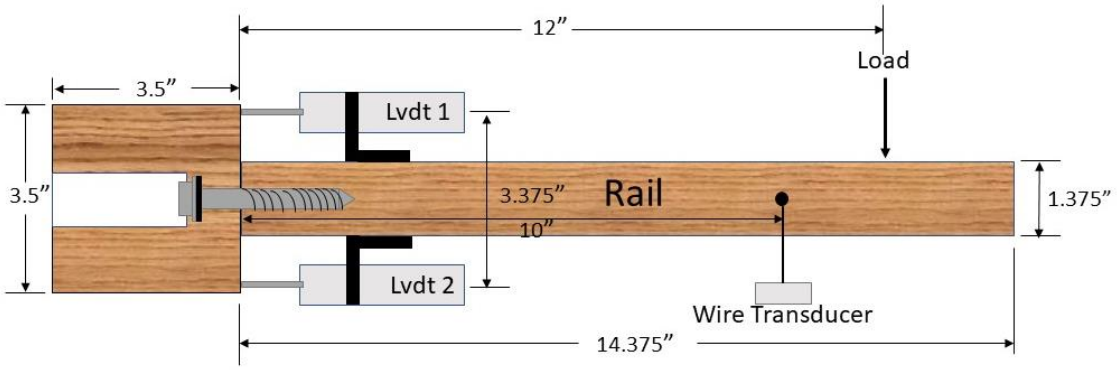

Figure 2.5 Simplified test setup along with instrumentation for measurements

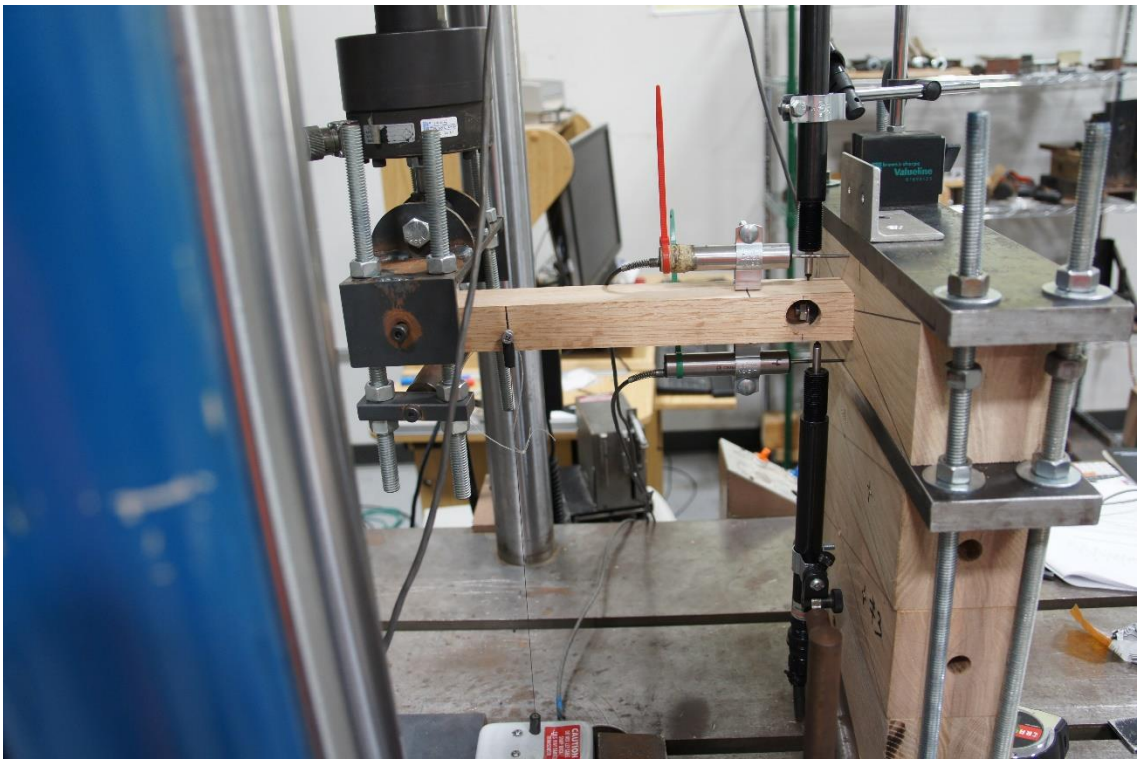

Figure 2.6 Test setup

2.3.4.2 Monotonic Loading

The monotonic tests were conducted based upon the guidelines found in EN 26891:1991 (CEN 1991). The maximum moment capacity of each joint configuration was determined in the static loading tests. Ten joints (C1-M-1, C1-M-2, C1-M-3, C1-M-4, C1-M-5, C2-M-1, C2-M-2, C2-M-3, C2-M-4, C2-M-5) were tested. Figure 2.7 shows a typical loading curve for the monotonic test as described in the standard. According to the standard a load is applied up to 40% of the estimated maximum load carrying capacity of the joint and maintained for 30 seconds. The load is then reduced back to 10% of the estimated maximum load capacity of the joint and maintained for 30 seconds. After this the load is increased unto the ultimate maximum load or a joint rotation of 0.15 rad. The loading rate below 70% of the estimated maximum capacity is 20% of the maximum load per minute ±25%. The loading rate above 70% is based

upon a constant rate of joint rotation such that the ultimate load or 0.15 rad joint rotation is reached in 3 to 5 minutes additional testing time. The load reached before (if there is a drop-in load) or at a joint rotation of 0.15 rad, shall be record as the maximum for each specimen.

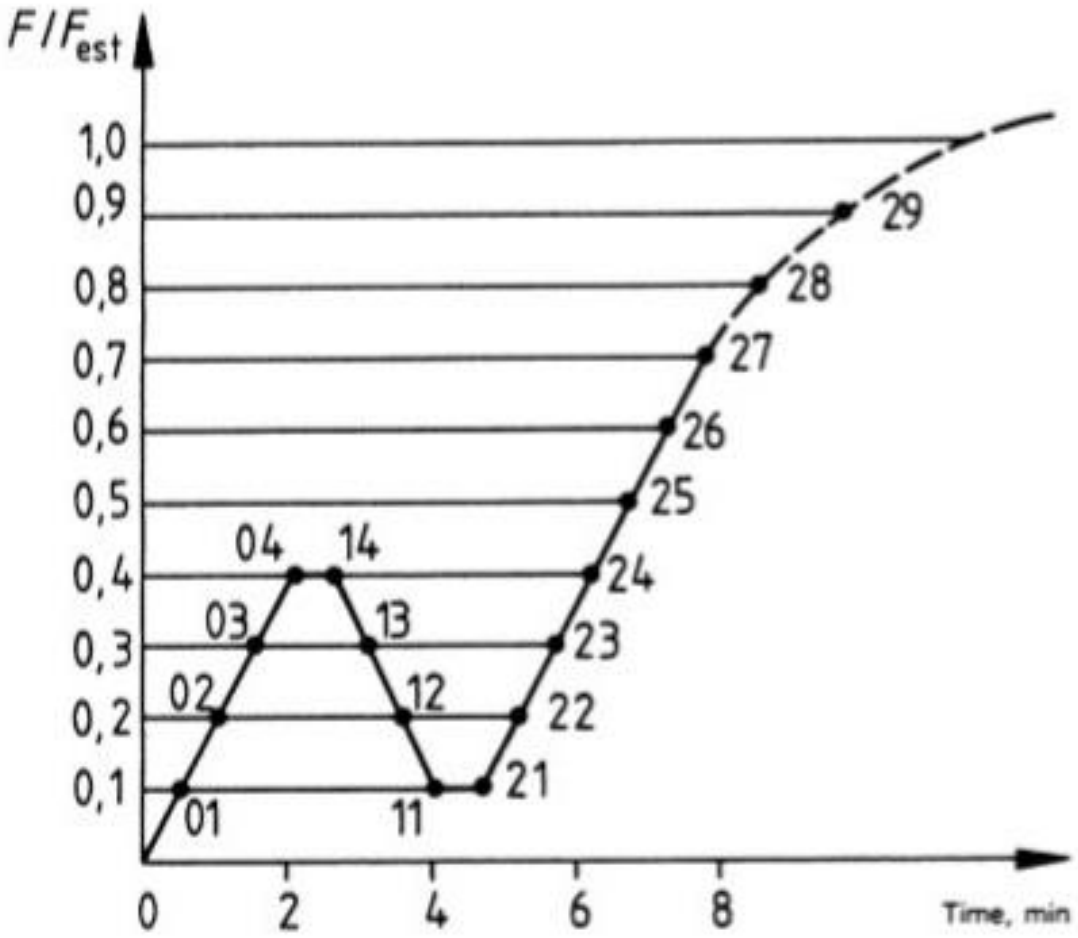

Figure 2.7 EN 26891:1991 Monotonic Test Loading Protocol

The curves generated from the monotonic load-displacement procedure found in EN 26891:1991 (CEN 1991) were used to define maximum moment, displacement at maximum moment, yield moment, and yield moment displacement. The slip modulus, moment carrying

capacity, energy dissipation, and ductility can be calculated from the curves. An example of M-Θ monotonic curve is shown in Figure 2.8.

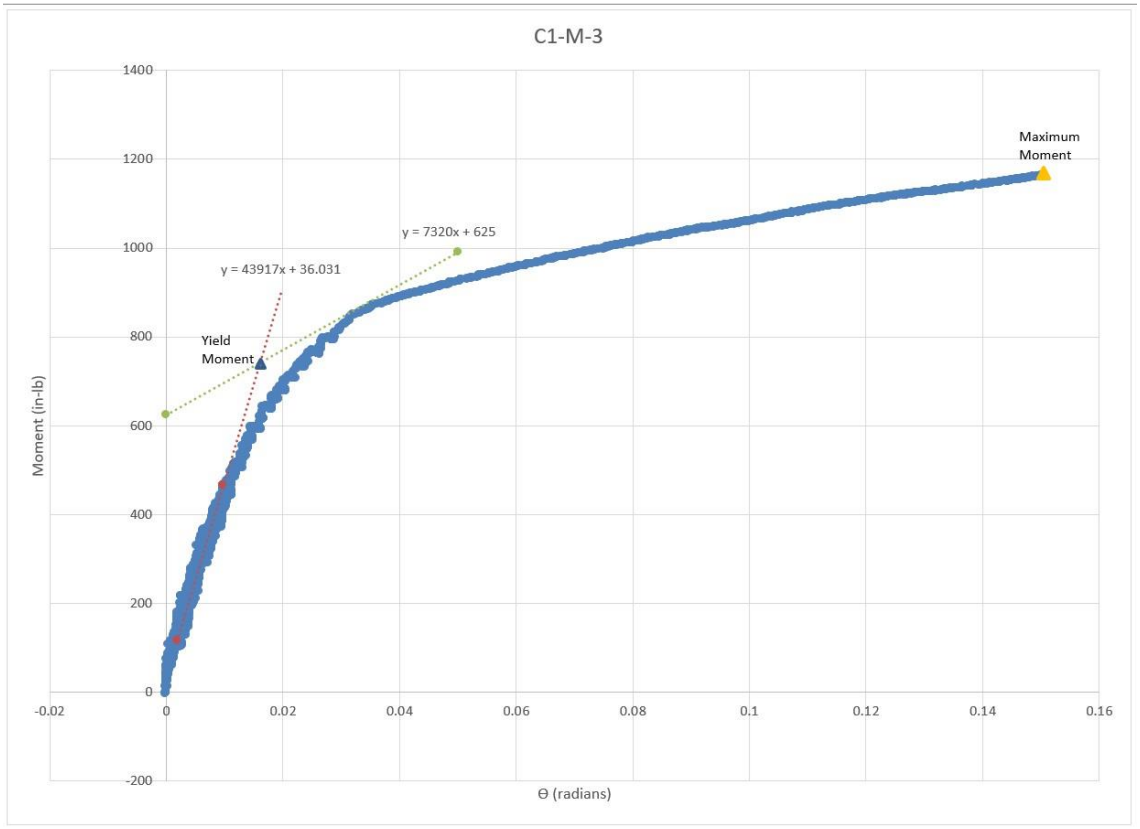

Figure 2.8 Monotonic M-Θ curve (Sample C1-M-3)

The maximum moment value was defined as a joint rotation of 0.15 rad if no moment drop had occurred. The purpose of setting the failure rotation to 0.15 rad involved the assumption that a 0.15 rad rotation was applicable to the 15 mm lateral slip failure as reported in EN 26891:1991 (CEN 1991). Awaludin et al. 2010 used this assumption when testing the moment resistance of timber joints with high-strength dowels reinforced with natural fiber.

The yield moment and yield displacement were calculated based upon the procedure in EN 12512:2001 (CEN 2001). This procedure defines the yield point as the intersection of two

lines. The first line corresponds to a line drawn starting at the first point at 0.1 M_{max} and then drawing the line connecting to the point corresponding to 0.4 $M_{max.}$ The second line is tangent with 1/6 of the first line's slope.

The initial stiffness was calculated by using 10% and 40% of the maximum moment and using the corresponding rotations according to EN 26891:1991 (CEN 1991), taking the estimated moment and modified initial slip, as expressed in equation 2.2:

$$\text{ks} = \frac{0.4Mmax - 0.1\ Mmax}{v04 - v01} \tag{2.2}$$

where k_s is equal to initial torsional stiffness (in-lbf/radians), M_{max} is equal to the maximum moment (in-lb), and v_{04} and v_{01} are the rotations (radians) corresponding to 0.4 and 0.1 M_{max}, respectively.

Ductility is the ability of the connection to endure the plastic region with a large deformation without considerable decrease in strength. Ductility can be calculated by dividing the maximum rotation by the yield rotation (Equation 2.3).

$$\text{D} = \frac{\text{Vm}}{\text{Vy}} \tag{2.3}$$

where D is equal to ductility; V_m is equal to maximum rotation (radians) or 0.15 rad whichever is less; and V_y is equal to yield rotation (radians).

2.3.4.3 Reversed-Cyclic Loading

The reversed-cyclic tests were conducted based upon the guidelines found in EN 12512:2001 (CEN 2001). The loading protocol values for this testing were also determined from preliminary tests. Ten joints (C1-C-1, C1-C-2, C1-C-3, C1-C-4, C1-C-5, C2-C-1, C2-C-2, C2-C-

3, C2-C-4, C2-C-5) were tested. Figure 2.9 shows a typical loading curve for the reverse-cyclic test. A load was applied in compression up to 25% of the estimated joint yield rotation and then unload and reload the joint in tension to zero-rotation.

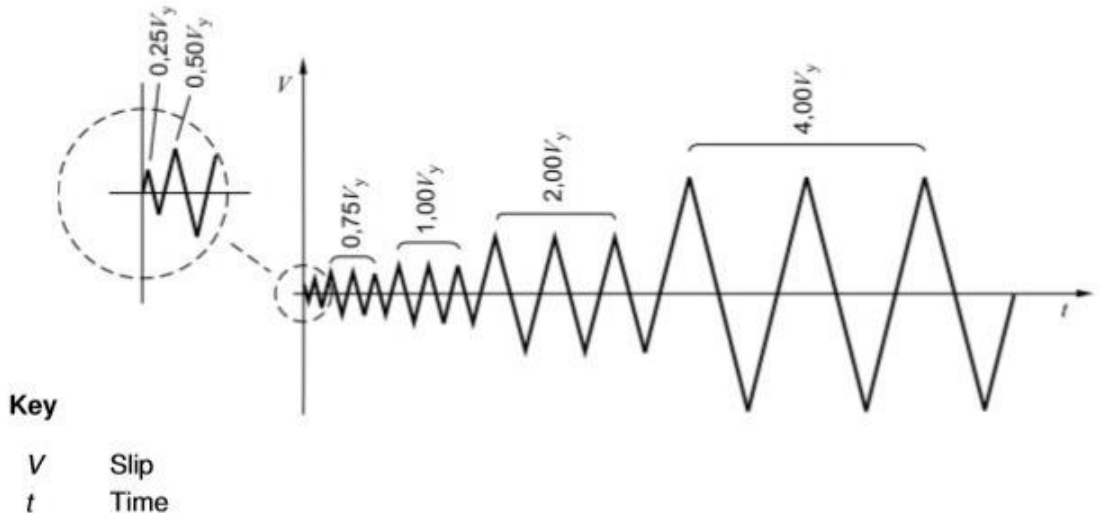

Figure 2.9 EN 12512:2001 Reverse Cyclic Test Loading Protocol

The load was the applied in tension up to 25% of the estimated joint yield rotation in tension and then unload the joint and reload it in compression to zero-slip. This is the 1st cycle. The 2nd cycle is a repeat of the first cycle, but with the applied loads reaching 50% of the estimated joint yield rotation. The 3rd, 4th, and 5th cycles consist of a repeat of first cycle, but with the applied loads reaching 75% of the estimated joint yield rotation. The 6th, 7th, and 8th cycles also consist of a repeat of first cycle, but with the applied loads reaching 100% of the estimated joint yield rotation. Cycles above the 8th cycles are also a repeat of the first cycle in sets of three cycles corresponding to applied loads of 200%, 400%, 600%, etc. of the estimated joint yield rotation. Testing is continued until joint failure or a joint rotation of 0.15 rad.

Reversed cyclic hysteresis curves obtained by following EN 12512:2001 (CEN 2001) loading protocol was used for reversed cyclic data analysis. Figure 2.10 shows an example of a hysteresis curve.

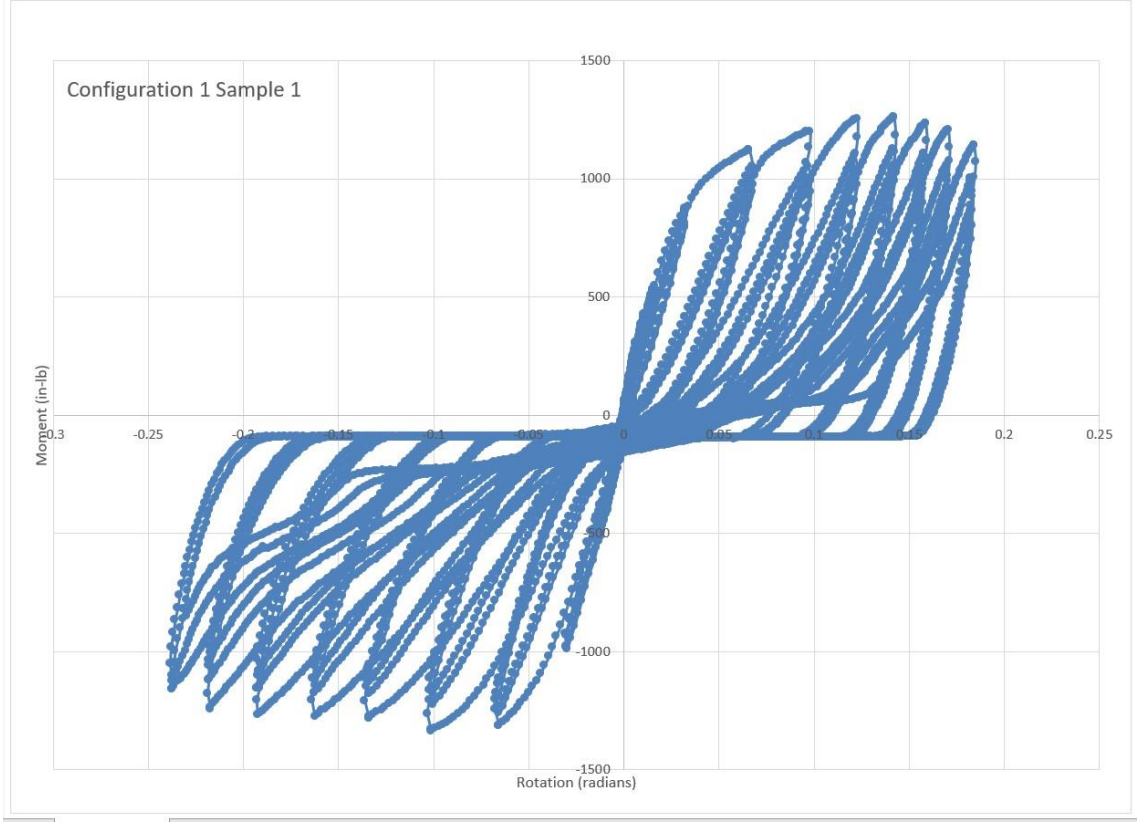

Figure 2.10 Example of hysteresis curve obtained by following EN 12512:2001 (Sample C1-C-1)

The negative and positive envelope curves were collected from the hysteresis curves. An average envelope curve was obtained from the negative and positive envelope curve for each sample so that the maximum moment, rotation at maximum moment, yield moment and yield rotation could be measured, following procedures proposed in ASTM E2126-19 (ASTM 2019). Figure 2.11 shows an example of an envelope curve.

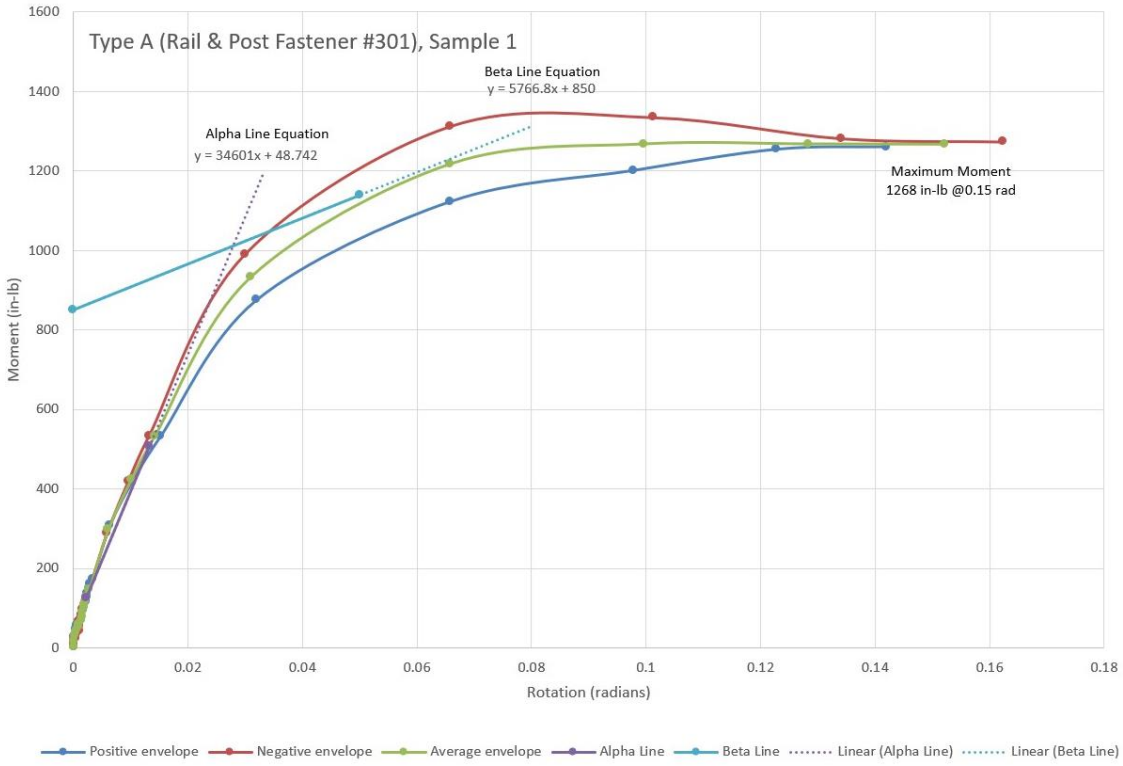

Figure 2.11 Example of envelope curves (Sample C1-C-1)

2.3.5 Statistical Analysis

The effects of two single metal dowel connection systems on the stiffness, yield moment strength, yield rotation, maximum moment, and ductility in a post-to-rail connection system under monotonic and reverse-cyclic loading was studied. The data was analyzed using SAS version 9.4. The assumption of normality and homogeneity of variance were tested on the raw data using the Shapiro-Wilk test and Levene's test, respectively. If the assumptions were not meet, the data was transformed by logarithmic-transformation, i.e. log(x), and tested again for normality and homogeneity of variance. If the data could not be normalized, the Kruskal-Wallis H test, a non-parametric equivalent of ANOVA was used to analyze the significance of the main effects. If the main effects proved to be significant at $\alpha = 0.05$, then mean rank separation was

done using Dunn's pairwise test adjusted by the Bonferroni correction. The Dunn's test is the specified test for nonparametric pairwise multiple-comparison procedure when a Kruskal-Wallis test is rejected. If assumptions of normality and homogeneity of variance were satisfied ($p > 0.05$), a one-way ANOVA and the Tukey Honestly Significant Difference (HSD) test was performed for mean separation within the main effects.

2.4 Results and Discussion

2.4.1 Static Loading

Table 2.1 presents the results for the static loading. The mean initial rotational modulus stiffness of rail-post fastener #301 was measured to be greater than the mean initial rotational modulus stiffness of the rail-bolt fastener #302. A 3/8" lag screw for #301 specimens was in full contact with a rail member, while a gap was formed between the 7/16" (diameter) clearance hole of the post member. For the #302 specimens, a gap was formed between the 3/8" (diameter) clearance hole of the rail and the 5/16" (diameter) hanger bolt. It was determined that the hole drilled into the end grain of the rail for the rail-bolt fastener #302 allowed for more lateral movement of the bolt within the hole during testing. This lateral movement within the hole could explain the reduction in the stiffness as compared to the rail-post fastener #301. Dong et al. (2021) showed that connections using dowel fasteners with oversized predrilled holes had low initial stiffness.

Table 2.1 Rotational resistance performance parameters descriptive statistics for #301 (C1) and #302 (C2) connection systems under static loads

		N	Mean	Std Deviation	Coefficient of Variation	Min	Max
Maximum Moment (in-lb)	C1	5	1,245	158	12.7	1,066	1,477
	C2	5	1,462	132	9.0	1,292	1,621
Rotation at Maximum Moment (radians)	C1	5	0.249	0.100	40.2	0.089	0.351
	C2	5	0.266	0.085	32.0	0.177	0.394
Yield Moment (in-lb)	C1	5	785	123	15.7	576	899
	C2	5	976	103	10.6	847	1.111
Yield Rotation (radians)	C1	5	0.017	0.003	18.1	0.013	0.020
	C2	5	0.038	0.008	21.5	0.026	0.047
Initial Stiffness (in-lb/radians)	C1	5	43,643	7,336	16.8	34,797	50,427
	C2	5	23,355	5,457	23.4	18,765	31,607

*The yield point on the moment-rotation curve represents the location where the joint's structural behavior becomes plastic from elastic. It is calculated following the procedure in EN 12512:2001. The yield points were defined as the intersection of two lines. The slope of the first line was determined from the line drawn from 10% of maximum moment to 40% of maximum moment and the second line being a tangent line to the moment-rotation curve with a slope 1/6 of the first line.

The mode of failure for the rail-post fastener #301 connector was noticed to be compression in the side grain of the post from both the rail and the compression of the washer on the bolt also into the side grain of the post (Figure 2.12a and Figure 2.12b). According to the wood handbook (Wood Handbook, 2021) the compression strength of red oak perpendicular to the grain is 870 psi at 12% MC. If the rail-post fastener #301 is located at the center of the rail, the top portion of the rail will be in tension and the bottom portion will be in compression. The area of the rail under the bottom side of the connection would be 1.375 in^2. Assume the average maximum moment for the rail-post fastener #301 is 1,200 in-lb. (100 pounds * 12 in.), the compression stress at the post would be approximately 872 psi (1,200 lb. / 1.375 in^2). The 872 psi is approximately the published compression strength of red oak perpendicular to the grain (Wood Handbook, 2021). The area of the washer within the post was measured to be 0.3973 in^2. Assuming that the average maximum moment is 1,200 in-lb., the compression stress in the post

at the washer would be approximately 3,020 psi. This stress exceeds the published compression stress perpendicular to the grain of red oak by approximately 3.5 times. This would explain the wood compression failure under the washer in the post.

a) b)

Figure 2.12 Perpendicular-to-grain compression failure examples for #301 (C1) post members in contact with a) rail members and b) lag screw washers

The mode of failure for the rail-bolt fastener #302 connector involved the compression of the serrated nut into the plastic washer in the rail and the compression in the side grain of the post on the bottom side (Figure 2.13a and Figure 2.13b). The compression stress on the post would be the same as the rail-post fastener #301 if assuming the same average maximum moment of 1200 in-lb. The washer is plastic, but the actual type of plastic is undetermined. The area of the serrated nut compressing against the plastic washer within the rail was measured to be 0.286 in^2. Assuming the average maximum moment of 1,200 in-lb. the compression stress in the

rail at the washer would be 4,196 psi. The compression yield strength of some plastics is less than 4,196 psi (high-density polyethylene (HDPE) (2,900 psi)) (Mittal 2022).

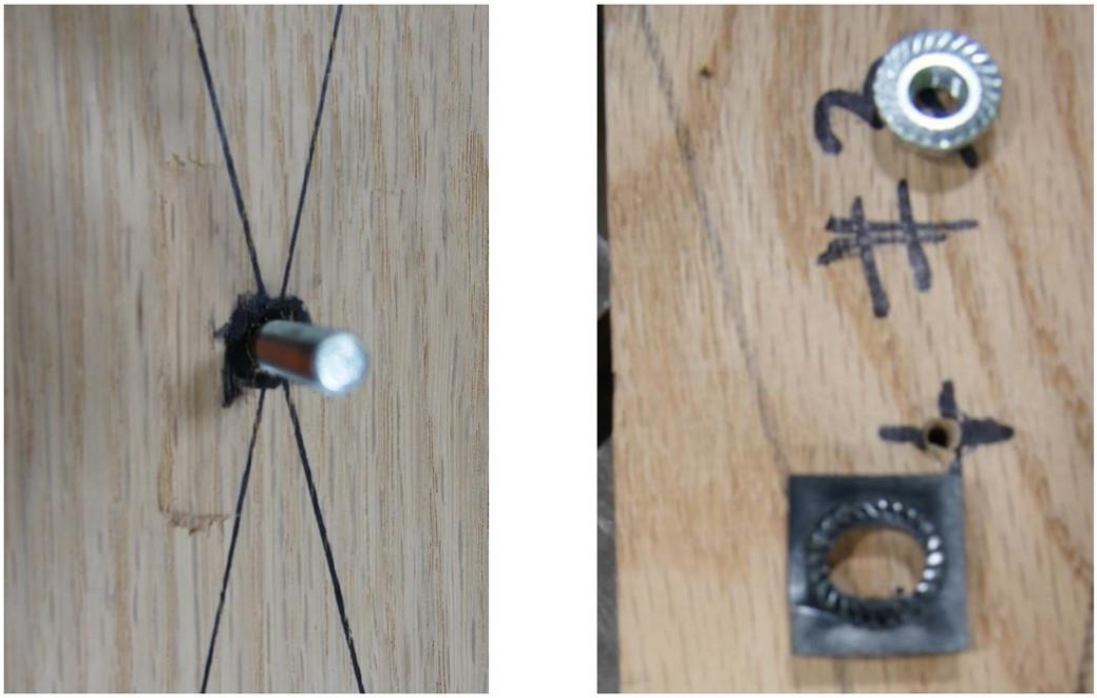

Figure 2.13 Perpendicular-to-grain compression failure examples for #302 (C2) post members in contact with a) rail members b) hanger bolt washers

Figure 2.14a and Figure 2.14b show a cut away view of the lag screw (rail-post fastener #301) on the rail member, and the hanger bolt (rail-bolt fastener #302) on the post member. No noticeable withdrawal of either connections was noticed in the wood members. The withdrawal strength of a lag screw is dependent upon the penetration depth, lag screw diameter, grain orientation, and wood density.

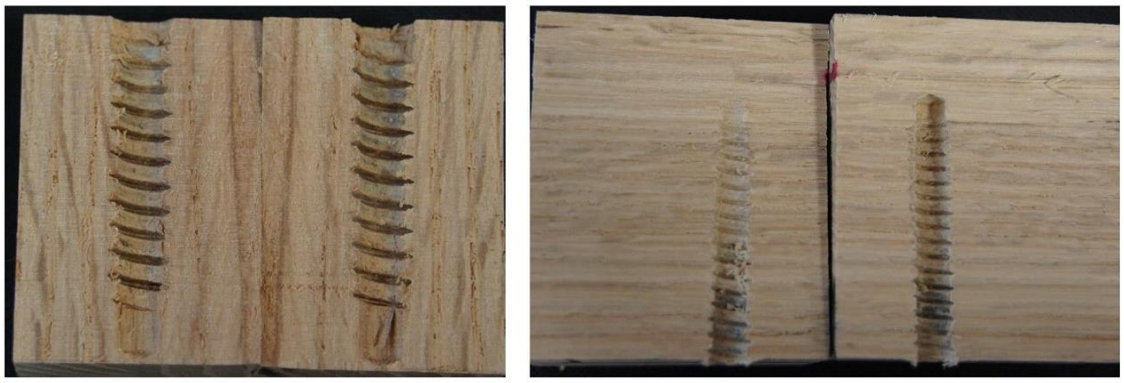

Figure 2.14 Cut views of a) #301 (C1) connection specimen's rail member and b) #302 (C2) connection specimen's post member, where a lag screw and hanger bolt were driven, respectively

2.4.2 Monotonic Loading

Tables 2.2 presents the results for the monotonic loading for the two connection systems. The modes of failure for the monotonic loading was consist with the modes of failure described in the static loading section. One of the specimens (C2-M5) experienced a split rail as the mode of failure. For the yield moment, yield rotation, and maximum moment, a one-way ANOVA was used to compare the two joint configurations since the datasets passed the normality and homogeneity of variance tests. There was no significant difference between the yield moment (Figure 2.15) and the max moment (Figure 2.16) for the two joint configurations. There was a significant difference between the yield rotation (Figure 2.17) of the two joint configurations with configuration #302 measuring a higher yield rotation. For the ductility, a one-way ANOVA was used to compare the two joint configurations on mean $\log_{10}$ductility values since the transformed datasets passed the normality and equality of variance tests. There was a significant difference between the ductility (Figure 2.18) of the two joint configurations with configuration #301 being more ductile than configuration #302. For the initial stiffness, the median initial

stiffness ranks for the two joint configurations were tested using the Kruskal-Wallis H test since the data could not be normalized even after transformation. There was a significant difference between the median initial stiffness ranks (Figure 2.19) of the two joint configurations.

Table 2.2 Rotational resistance performance parameters descriptive statistics for #301 (C1) and #302 (C2) connection systems under monotonic loads

		N	Mean	Std Deviation	Coefficient of Variation	Min	Max
Initial Stiffness	C1	5	50,776	8,693	17.1	39,203	59,216
(lb-in / radians)	C2	5	26,914	6,245	23.2	23,243	37,982
Yield Moment	C1	5	742	164	22.1	461	873
(lb-in)	C2	5	963	141	14.6	774	1,153
Yield Rotation	C1	5	0.0142	0.0041	29.1	0.00765	0.0186
(radians)	C2	5	0.0359	0.0104	29.0	0.0188	0.0457
Maximum	C1	5	1,182	173	14.6	904	1,353
Moment (lb-in)	C2	5	1,349	126	9.3	1,234	1,498
Ductility	C1	5	11.61	4.63	39.9	8.06	19.61
	C2	5	4.61	1.92	41.7	3.28	7.98

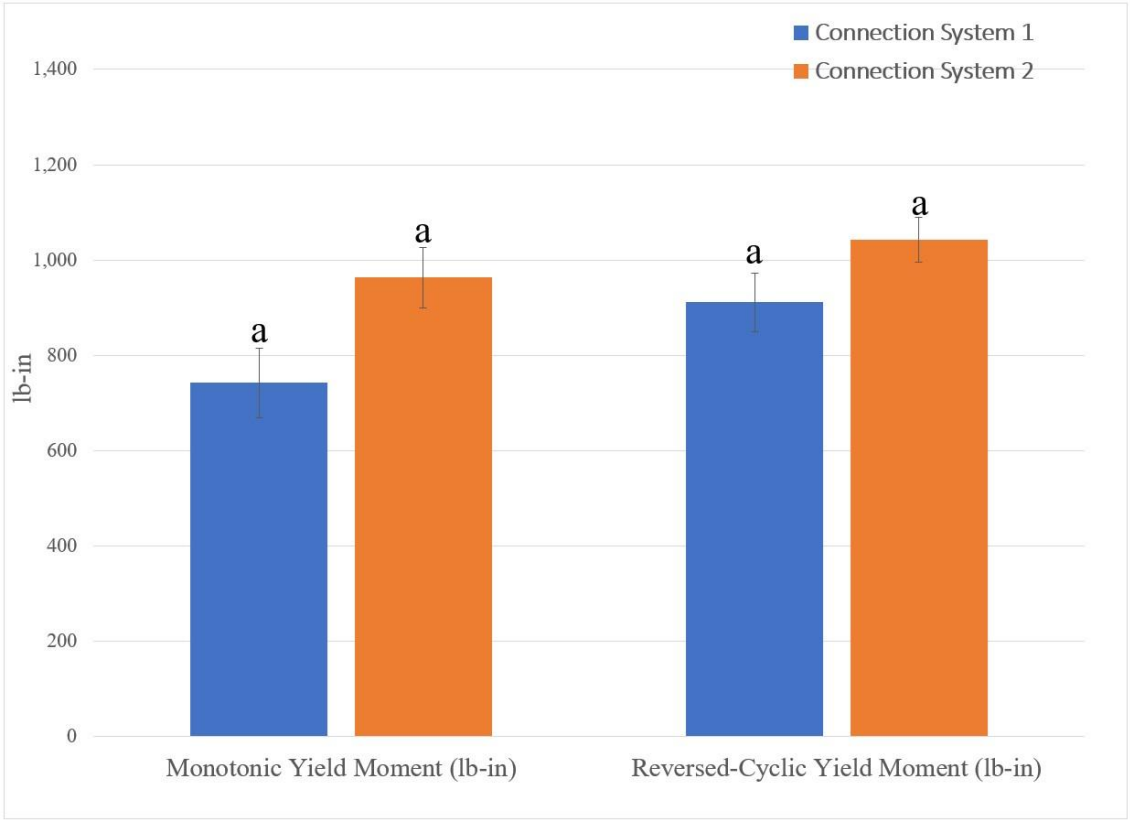

Figure 2.15 Mean yield moment of the #301 (C1) and #302 (C2) connection system under monotonic and reverse-cyclic loads (bars represent standard error; different letters above the bars indicate significant differences ($p<0.05$) among connection systems within a loading condition. Tukey HSD was used for the mean pairwise comparison

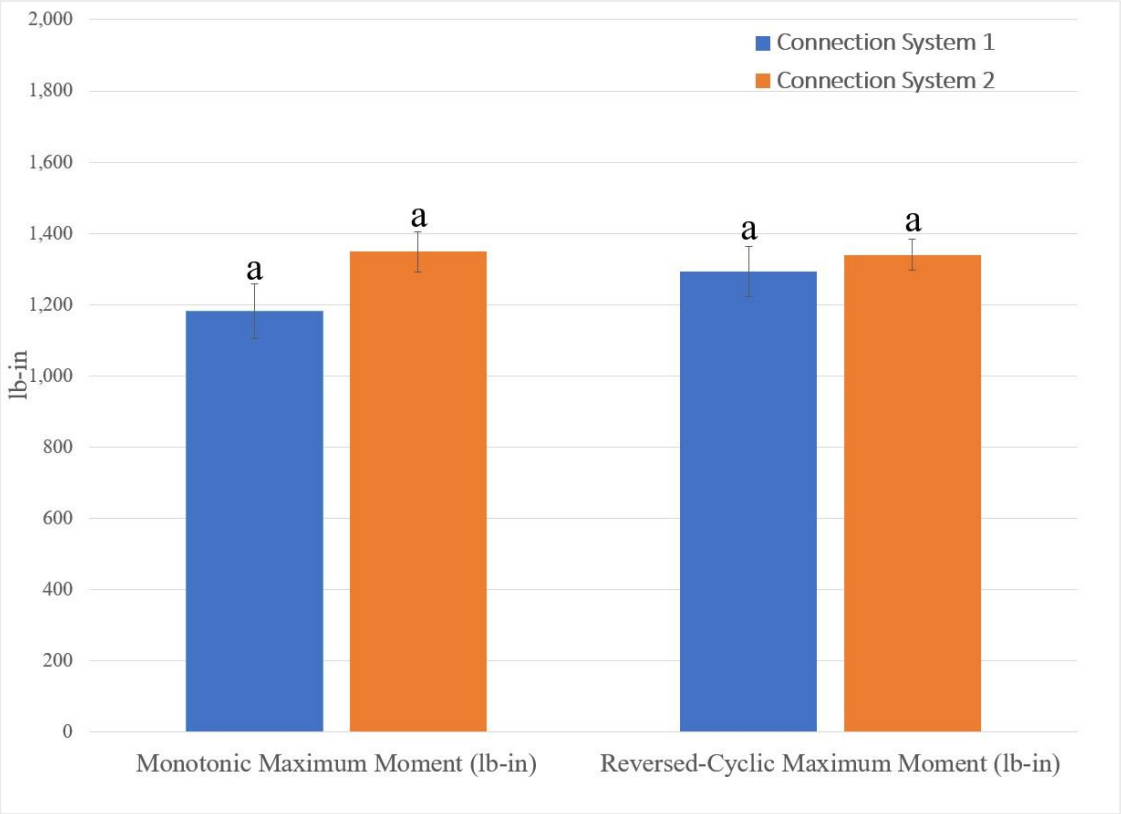

Figure 2.16 Mean maximum moment of the #301 (C1) and #302 (C2) connection system under monotonic and reverse-cyclic loads (bars represent standard error; different letters above the bars indicate significant differences ($p<0.05$) among connection systems within a loading condition. Tukey HSD was used for the mean pairwise comparison

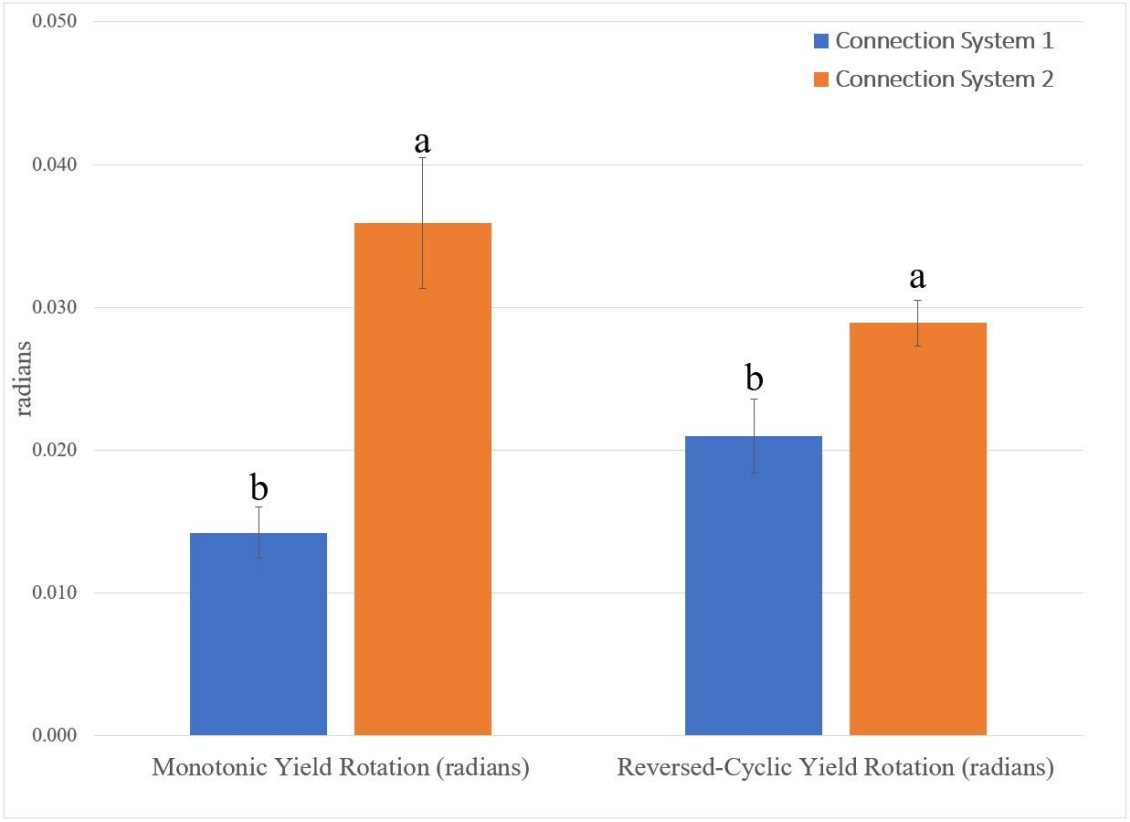

Figure 2.17 Mean yield rotation of the #301 (C1) and #302 (C2) connection system under monotonic and reverse-cyclic loads (bars represent standard error; different letters above the bars indicate significant differences ($p<0.05$) among connection systems within a loading condition. Tukey HSD was used for the mean pairwise comparison

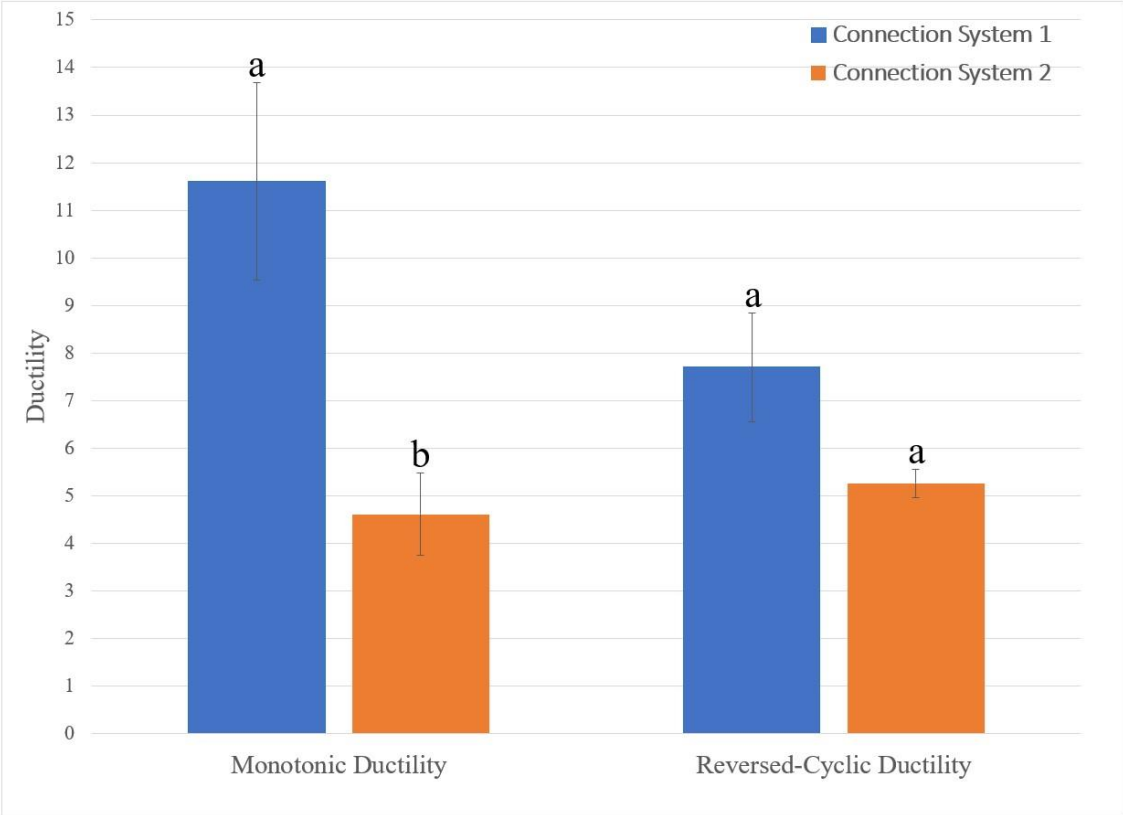

Figure 2.18 Mean ductility of the #301 (C1) and #302 (C2) connection system under monotonic and reverse-cyclic loads (bars represent standard error; different letters above the bars indicate significant differences ($p<0.05$) among connection systems within a loading condition. Tukey HSD was used for the mean pairwise comparison

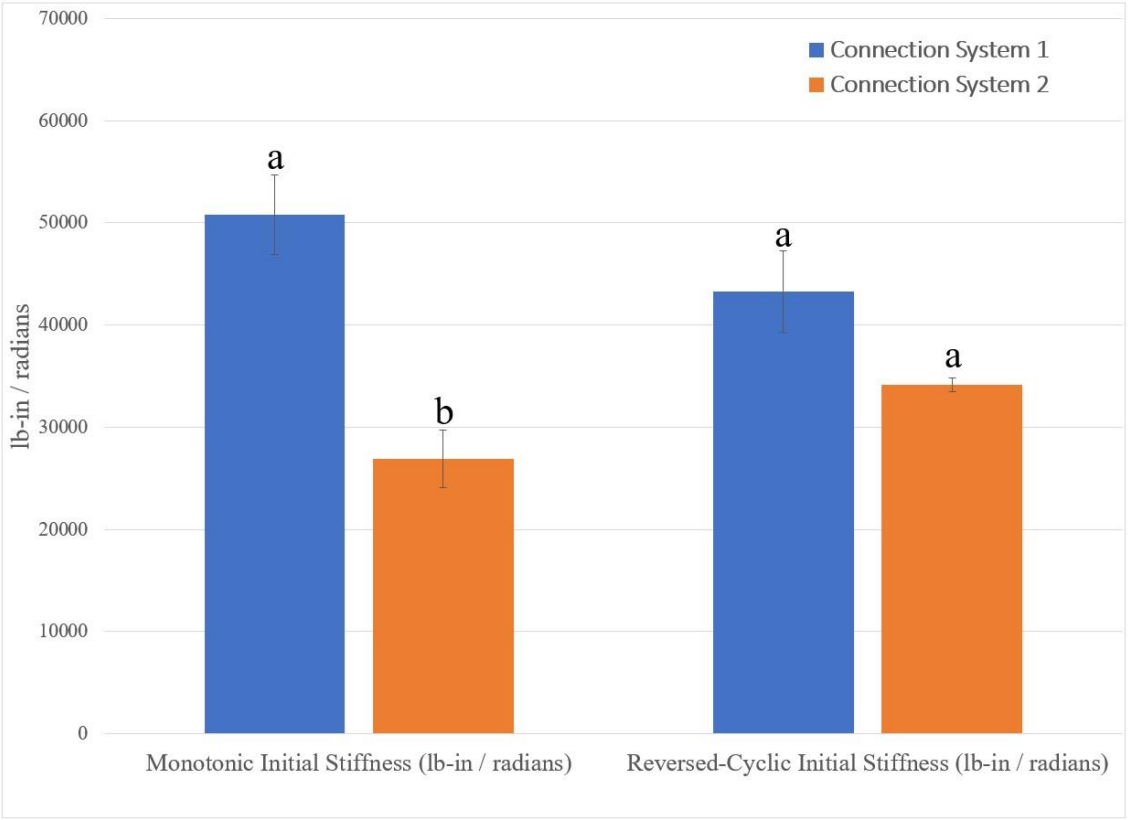

Figure 2.19 Mean initial stiffness of the #301 (C1) and #302 (C2) connection system under monotonic and reverse-cyclic loads (bars represent standard error; different letters above the bars indicate significant differences ($p<0.05$) among connection systems within a loading condition. Dunn's test with p-values adjusted by Bonferroni correction used for the mean pairwise comparison

2.4.3 Reversed-Cyclic Loading

Table 2.3 presents the results for the reversed-cyclic loading for the two connection systems. The modes of failure for the reversed-cyclic loading was consistent with the modes of failure described in the static loading section. For the yield moment, yield rotation, maximum moment, and ductility, a one-way ANOVA was used to compare the two joint configurations since the datasets passed the normality and equality of variance tests. There was no significant difference between the yield moment (Figure 2.15) and the maximum moment (Figure 2.16) for the two joint configurations. There was a significant difference between the yield rotation

(Figure 2.17) of the two joint configurations with configuration #302 measuring a significantly higher yield rotation. There was no significant difference between the ductility (Figure 2.18) for the two joint configurations. For the initial stiffness, the median initial stiffness ranks for the two joint configurations were tested using the Kruskal-Wallis H test since the data could not pass the equality of variance tests even after transformation. There was no significant difference between the median initial stiffness ranks (Figure 2.19) of the two joint configurations.

Table 2.3 Rotational resistance performance parameters descriptive statistics for #301 (C1) and #302 (C2) connection systems under reversed-cyclic loads

		N	Mean	Std Deviation	Coefficient of Variation	Min	Max
Initial Stiffness	C1	5	43,288	8,865	20.5	34,398	54,755
(lb-in / radians)	C2	5	34,135	1.456	4.3	32,581	35,905
Yield Moment	C1	5	911	138	15.1	715	1,035
(lb-in)	C2	5	1,042	105	10.0	903	1,183
Yield Rotation	C1	5	0.021	0.0058	27.4	0.0126	0.0278
(radians)	C2	5	0.0289	0.0036	12.3	0.0245	0.0323
Maximum	C1	5	1,292	157	12.2	1,124	1,469
Moment (lb-in)	C2	5	1,340	96	7.1	1,192	1,446
Ductility	C1	5	7.70	2.55	33.1	5.4	11.9
	C2	5	5.26	0.67	12.8	4.64	6.12

2.5 Conclusion

This study examined the monotonic and cyclic behavior of the moment resisting performance of two different type of concealed single-bolt connectors linking the post-to-handrail of a stairway guard system. The main components of the two systems were a 3/8” lag screw and a 5/16” hanger bolt. The joint with the 3/8 lag screw measured a higher initial stiffness than the 5/16” hanger bolt joint, but it was only significantly higher statistically for the monotonic loading conditions. There was no difference in the yield strength of the joints regardless of the loading conditions (monotonic or reversed-cyclic), but the yield rotation was

significantly more for the 5/16” hanger bolt joint for both loading conditions. The modes of failure were similar for both joints being compression of the wood on the post and the rail.

2.6 References

American Society for Testing and Materials. 2019. E 2126. Standard Test Methods for Cyclic (Reversed) Load Test for Shear Resistance of Vertical Elements of the Lateral Force Resisting Systems for Buildings. ASTM International. West Conshohocken, PA.

American Society for Testing and Materials. 2020. D 4442. Standard Test Methods for Direct Moisture Content Measurement of Wood and Wood-Based Materials. ASTM International. West Conshohocken, PA.

Awaludin A, Sasaki Y, Oikawa A, Hirai T, and Hayashikawa T. 2010. Moment Resisting Timber Joints with High-Strength Steel Dowels: Natural Fiber Reinforcements. In: World Conference on Timber Engineer, WCTE 2010. 20-24 June 2010; Trento, Italy. 4pp.

Bauchau OA and Craig JI. 2009. Euler-Bernoulli Beam Theory. Structural Analysis. Solid Mechanics and Its Applications. Vol 163. Sprinter, Dordrecht

Dong W, Li M, He M, Li Z. 2021. Experimental Testing and Analytical Modeling of Glulam Moment Connections with Self-Drilling Dowels. Journal of Structural Engineering 147(5):1-7.

European Committee for Standardization (CEN) (1991). EN 26891. Timber Structures, Joints made with Mechanical Fasteners, General Principles for the Determination of Strength and Deformation Characteristics. Brussels, Belgium.

European Committee for Standardization (CEN) (2005). SS-EN 12512/A1. Timber Structures, Test Methods, Cyclic Testing of Joints made with Mechanical Fasteners. Comite Europeen De Normalization, Brussels, Belgium.

Maki BE. 1985. Influence of Handrail Shape, Size and Surface Texture on the Ability of Young and Elderly Users to Generate Stabilizing Forces and Moments. Technical Report Number 29401. National Research Council of Canada, Ottawa.

Mittal A. 2022. What is Compressive Strength of Plastics. https://plasticranger.com/what-is-compressive-strength-of-plastics-the-complete-guide/#Difference_Between_Compressive_Strength_and_Compressive_Modulus. (31 January 2023).

Pencik J. 2015. Analysis of Support of Stairs in a Wooden Prefabricated Staircase with One-sided Suspended Stairs Made from Scots Pine (*Pinus Sylvestris*) with the use of Experimental Tests and Numerical Analysis. Wood Research 60(3):477-490.

Pousette A. 2006. Testing and Modeling of the Behavior of Wooden Stairs and Stair Joints. Journal of Wood Science 52:358-362.

SAS Institute. 2016. SAS software, version 9.4. The SAS Institute Inc. Cary, NC.

Senalik CA and Farber B. 2021. Mechanical Properties of Wood. Pages 5.1-5.46, Wood Handbook. USDA Forest Service. Forest Products Laboratory. FPL-GTR-190. Madison, WI.

Templer J, Archea J, and Cohen HH. 1985. Study of Factors Associated with Risk of Work-Related Stairway Falls. Journal of Safety Research 16(4):183-196.

CHAPTER III

DEVELOPMENT OF PRESERVATIVE-TREATED CROSS-LAMINATED TIMBER: EFFECTS OF PANEL LAYUP AND THICKNESS ON BONDING PERFORMANCE AND DURABILITY WHEN TREATED WITH COPPER-AZOLE (CA-C) AND MICRONIZED COPPER-AZOLE (MCA)

3.1 Abstract

Cross-laminated timber (CLT) has proven to be a promising construction material because of its mechanical properties, low carbon footprint, and sustainability as compared to steel and concrete. The susceptibility of CLT to biodeterioration limits its use to interior or protected applications. To expand the use of CLT to exterior applications, a need to investigate methods to treat CLT has emerged. Pressure treatments are effective methods of increasing the durability of wood products; however, studies on pressure treated CLT is limited. In this study, preservative-treated CLT from prefabricated CLT panels was prepared and impregnated with Cu-based preservatives through a conventional vacuum process. The effects of panel layup (longitudinal and crosswise), thickness (3- and 5-layer), and preservative treatment (CA-C and MCA) on bonding performance were investigated. The bonding performance of post-treated southern yellow pine CLT panels was evaluated using block shear and delamination tests by referencing ASTM D905 and ASTM D2559 Standards, respectively. Panel layup, thickness, and preservative treatment did have an influence on the block shear strength (BSS) and percentage of wood failure (WFP) of the treated panels. Approximately 60% of the block shear specimens

passed the minimum WFP requirement of 75% specified in ASTM D2559. Less than 10% of the delamination specimens passed the allowable delamination rate of 1% specified in ASTM D2559. The low percentage of wood failure and the low percentage of specimens passing the allowable delamination rate could have been influenced by the air drying of the CLT panels from approximately 85% MC to 20% MC, and cohesive failure of the adhesive was observed in control specimens. The post treating of CLT panels with CA-C or MCA with a PUR adhesive has potential if the panels could remain in the green condition or if a feasible kiln drying cycling can be utilized. No noticeable delamination of the panels was observed during the actual treating phase of the study.

3.2 Introduction

Cross-laminated timber (CLT) is an engineered wood product (EWP) manufactured mainly from softwood dimension lumber or structural composite lumber. Adjacent layers are typically bonded in layers at 90° to each other, similar to plywood. The wood laminates are bonded by adhesive, nails, wooden dowels, or a combination thereof. CLT panels are typically manufactured with 3 to 9-layers. CLT was first developed in European countries of Austria and Germany in the 1970s and 1980s. CLT has enjoyed a major level of success in the European construction market and is establishing a presence in North American construction projects (Brandner et al. 2016).

In order to expand the use of CLT in exterior applications the question about durability must be addressed when exposed to moisture (weathering), decay, and wood-attacking insects such as termites. CLT panels are usually covered for protection from the environment when transported from the manufacturing company to the construction site. Weather resistant barriers (WRB) are used in building envelop system keep CLT panels dry. Gagnon and Pirvu (2011)

suggests the use of preservative treated CLT panels in an environment of high humidity and high termite risk especially when in close contact with the building foundation.

There are structural adhesive and preservative systems that are commercially available for producing durable structural wood composites. The panel bond quality, durability and mechanical properties can be determined through standardized testing specified in the CLT Handbook (2013). According to the CLT Handbook there are three adhesive groups that are used to manufacture CLT panels: phenolic and aminoplastic adhesive systems such as phenol-resorcinol formaldehyde (PRF), one-component polyurethane adhesive system (1C-PUR), and emulsion polymer isocyanate (EPI) system.

The preservative treating systems can be oil-solvent or water-based. Oil-based preservative systems are coal-tar creosotes and pentachlorophenol solutions. Preservative treating of wood using copper compounds for wood protection has been around for over 200 years (Nguyen et al. 2012). There are some brown-rot decay fungus species that can tolerant copper compounds. Other co-biocides are added to copper compound preservative systems to make effective against copper-tolerant fungus species (Freeman and McIntyre 2008). Within the US, the volume of wood products treated with copper-based preservatives grew exponentially during the 1970s and 1980s and remains high today (De Groot and Woodward 1999). Chromated copper arsenate (CCA) was once a popular preservative system for most residential applications until it was voluntarily withdrawn (January 1, 2004) because of possible health impacts because of the arsenic leaching into the environment (Townsend et al. 2005). CCA is still used for non-residential applications. To replace CCA for residential applications, preservative systems that are more environmentally friendly have been developed such as alkaline copper quaternary (ACQ) and copper azole (CA).

Adhan et al. (2020) constructed treated 3-ply single-species and mixed species CLT panels from four Malaysian hardwood species (batai, sesendui, rubberwood, and kedondong). There, hardwood laminates were preservative treated with a 2% alkaline copper quaternary (ACQ) solution and bonded with phenol-resorcinol-formaldehyde resin. The study included two different surface pressures (0.7 MPa and 1.4 MPa) and three different glue spread rates (200 g/m^2, 250 g/m^2, and 300 g/m^2). For the single CLT configuration the treated rubberwood measured the highest shear strength of 9.53 MPa while batai measured the lowest at 4.19 MPa. The preservative treatment had no significant effect on block shear strength (BSS) and no noticeable visible delamination.

Lee et al. (2006) using ASTM D905 reported on the dry BSS of two softwood species (Korean pine and Japanese larch) treated with four levels of waterborne preservatives (untreated; CCA, CD-HDO (copper, boric acid, and N-cyclohexyldizeniumdioxide); and CA) bonded together with four different adhesive systems (urea-melamine formaldehyde, UMF; melamine formaldehyde, MF; phenol formaldehyde, PF; and resorcinol formaldehyde, RF). The dry shear values ranged from 0.52 MPa to 5.50 MPa with no evident trends.

Lisperguer and Becker (2005) compared the bond strength durability of two different adhesives (commercial and laboratory-modified PRF) when bonding radiata pine wood treated with different retention levels (4 and 6 kg/m^3) of chromated copper arsenate (CCA). The modified PRF passed the minimum requirements for ASTM D2559 which was < 1% delamination rate.

Lim et al. (2020) measured the block shear strength (BSS) and delamination rate of 3-ply southern yellow pine CLT panels fabricated from micronized copper azole-type C (MCA-C) lumber treated to 1.0 kg/m^3 and 2.4 kg/m^3 preservative retention levels bonded with three

different adhesive systems. The results showed that BSS and delamination rate was influenced by preservative treatment and the adhesive system. Lim et al. successfully fabricated 3-ply southern yellow pine (SYP) CLT panels from micronized copper azole type C (MCA-C) preservative system using three different adhesive systems (melamine formaldehyde, resorcinol formaldehyde, and one component polyurethane.

There is a lack of data on the effects of post treatment of southern yellow pine CLT panels when treated with micronized copper azole (MCA) or copper azole-type C (CA-C) to the retention level of 2.4 kg/m^3 (UC4A (ground contact or fresh water) applications specified by AWPA Standard U1-18) on the adhesive performance. The adhesive was a one component polyurethane, PUR. MCA and CA-C are both commercial preservative systems for pressure treated lumber for residential applications.

3.3 Materials and Methods

3.3.1 Materials

Visually graded Select Structural (SS) southern yellow pine (SYP) lumber (38.1 mm x 139.7 mm x 2438.4 mm) was supplied by a regional sawmill. The SS lumber was chosen in order to minimize lumber defects as specified in the Southern Pine Grading Rules (SPIB 2014). Each piece of lumber was weighed with an electronic scale and placed into one of four weight classes. The weight classes follow: 1) < 6,000, 2) 6,000 grams to 7,000 grams, 3) 7,000 grams to 8,000 grams, and 4) > 8,000 grams. This sorting was done to control the lumber density range for the laminates minimized the variability within samples. The wood laminates for CLT construction were cut from lumber in weight classes 2 and 3. The clear wood sections of the lumber was labeled and divided into 762 mm and 508 mm sections. As specified in ASTM D2559 (2017) only flat-grain (wood with growth rings that make an angle < 45° with the wide surface)

laminates with no pith were chosen as laminates. The wood laminates were planed on each face to a final thickness of 35.6 mm before gluing. SG and MC specimens were cut from each section according to ASTM D2395 (2017) and ASTM D4442 (2020), respectively. Table 3.1 shows the average MC and the oven-dry specific gravity ($SG_{oven\text{-}dry}$) of the laminates. The average specific gravity of the laminates was 0.49 with an average moisture content of 11.89%.

Table 3.1 Summary statics of MCs and SGs of lumber laminates used in CLT fabrication.

		Moisture Content (%)			Specific Gravity$_{oven\text{-}dry}$		
		Mean	SD[a]	COV[b]	Mean	SD	COV
3-layer parallel CLT	Control	10.78	1.36	12.67	0.52	0.03	5.35
	CA-C	11.19	1.22	10.91	0.50	0.04	8.90
	MCA	13.04	1.60	12.30	0.48	0.04	7.51
3-layer perpendicular CLT	Control	10.77	1.09	10.13	0.51	0.02	3.89
	CA-C	11.28	1.13	10.01	0.48	0.04	9.32
	MCA	12.02	0.86	7.19	0.47	0.03	7.21
5-layer parallel CLT	Control	10.70	0.82	7.70	0.50	0.04	7.02
	CA-C	13.98	1.10	7.88	0.46	0.03	7.33
	MCA	13.19	1.18	8.93	0.46	0.03	6.21

Note: [a]SD means standard deviation, [b]COV means coefficient of variation.

3.3.2 CLT manufacturing

The adhesive used for this study was a single-component polyurethane adhesive (LOCTITE PUR HB X602), supplied by Henkel Corporation. Before applying the adhesive, a wood primer was sprayed (spreading rate of 20 g/m^2) onto the surface of the wood at least 10 minutes before adhesive application. The wood primer used was LOCTITE PR 3105 (specifically for bonding southern pine), also supplied by Henkel Corporation. The primer was mixed with tap water before use at the concentration of 10% by weight (9 parts by weight of tap water and 1 part by weight of primer). After the 10-minute curing of the primer on the wood surface, the PUR adhesive was applied with a spreading rate of 180 g/m^2 according to adhesive

product specifications. The CLT panels were fabricated within 8 hours of the laminates being planed.

Three CLT panel configurations used for this study are shown in Figure 3.1. Configurations 1 and 2 were 3-ply, while Configuration 3 was 5-ply construction. The main difference between Configuration 1 and 2, was that Configuration 1 has the top and bottom layers laminates parallel to the panel long direction with the middle layer laminates perpendicular to the panel long direction. Configuration 2 consisted of the top and bottom layers laminates perpendicular to the panel long direction with the middle layer laminates parallel to the panel long direction. Configuration 3 consisted of the top, middle, and bottom layer laminates parallel to the panel long direction with the other two-layer laminates perpendicular to the panel long direction. The parallel layers were composed of three laminates (edge to edge) while the perpendicular layers were composed of five laminates (edge to edge). The final panel dimensions were 404 mm x 676 mm x 104 mm for the 3-ply CLT panel. The final panel dimensions were 404 mm x 676 mm x 175 mm for the 5-ply CLT panel.

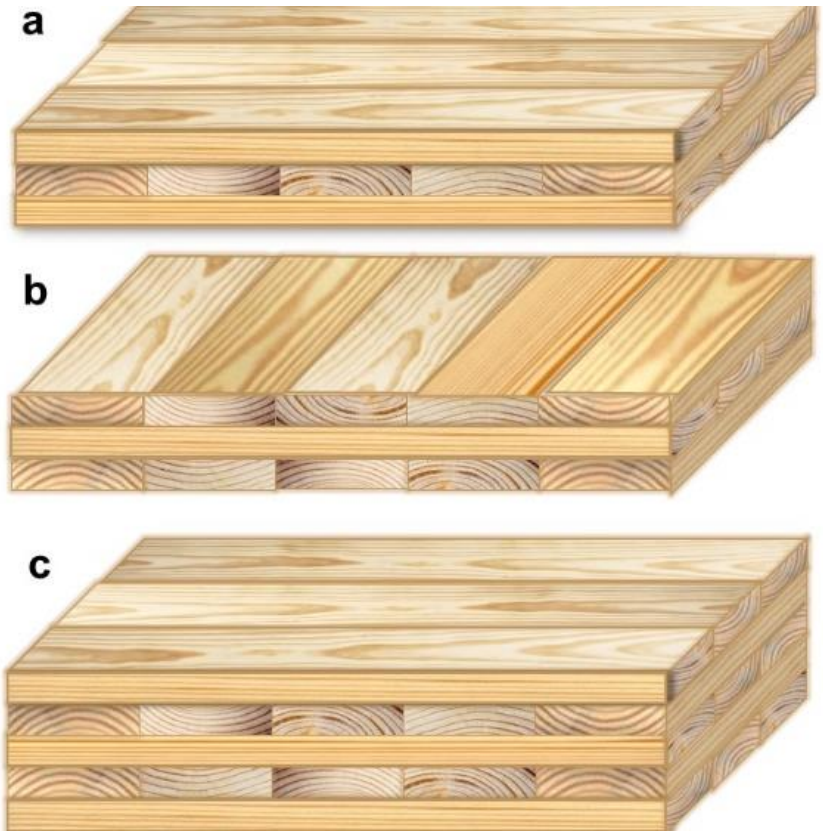

Figure 3.1 CLT panel configurations (a) 3-ply, longitudinal, LT, (b) 3-ply, crosswise, CS, and (c) 5-ply, longitudinal, LT

The panels were manufactured using a Dieffenbacher laboratory hydraulic press (Figure 3.2). The pressing parameters for the panels follow: Step 1 – Press 0.207 MPa for 1 minute, Step 2 – Press 0.345 MPa for 1 minute, Step 3 – Press 0.689 MPa for 180 minutes, and Step 4 – Press 0.345 MPa for 0.5 minutes. A total of 27 panels were manufactured (10 CLT panels for Configuration 1, 10 CLT panels for Configuration 2, and 7 CLT panels for Configuration 3). The panels were sorted into three treatment groups and stored indoors until preservative treatment of the treatment groups.

Figure 3.2 3-ply CLT panels in Dieffenbacher laboratory hydraulic press

3.3.3 Preservative treatment of CLT

The three groups are as follows: copper azole - type C (CA-C) treatment group, micronized copper azole (MCA) treatment group, and an untreated control group. Eleven CLT panels were treated at Deforest Wood Preserving (1400 Industrial Drive, Bolton, MS) for the CA-C (Figures 3.3 to 3.5). Eleven CLT panels were treated at Koppers Performance Chemicals (1016 Everee Inn Road, Griffin, GA) for MCA (Figures 3.6 to 3.7).

The American Wood Protection Association (AWPA) Standards list the active ingredients for CA-C as 96.1% copper, 1.95% propiconazole, and 1.95% tebuconazole (AWPA 2017), and MCA as 96.1% copper and 3.9% tebuconazole (AWPA 2017). The panels were treated at the treating facilities according to 2-inch-thick dimension lumber protocols through a modified full-cell process. The modified full-cell process consisted of a shorter vacuum time than the normal full-cell process which has an initial vacuum of at least 30 minutes and above.

The target retention was 2.4 kg/m^3 for the panels. This retention level is specified by the AWPA U1-18 for UC4A (ground contact or freshwater) applications (AWPA 2018). Table 3.2 shows the preservative treating cycles as reported by the treating facilities. Both facilities confirmed the target retention of 2.4 kg/m^3 (Figure 3.8). After preservative treatment, the CA-C and MCA panels were allowed to air dry for 1 and 14 days, respectively, before being transported back to our laboratory. The treated and untreated panels were placed under the breezeway at the Franklin Center at Mississippi State University Department of Sustainable Bioproducts to air dry or absorb moisture as the case for the untreated panels (Figure 3.9).

Table 3.2 Preservative treating cycle.

	Preservative Treatment	
Parameters	CA-C	MCA
Initial Vacuum (in.-Hg)	18	18
Hold Time (minutes)	3	5
Pressure (MPa)	1.07	1.03
Hold Time (minutes)	11	15
Final Vacuum (in.-Hg)	20	26
Hold Time (minutes)	58	15

Figure 3.3 Eleven CLT panels ready for transportation to Deforest Wood Preserving in Bolton, MS for CA-C treatment

Figure 3.4 Charge of lumber coming out of treatment cylinder at Deforest Wood Preserving. CLT samples at the other end of treatment cylinder

Figure 3.5 CLT panels after CA-C treating at Deforest Wood Preserving

Figure 3.6 CLT panels prepared for shipment to Koppers Performance Chemicals in Griffin, GA for MCA treatment

Figure 3.7 CLT panels after MCA treating at Koppers Performance Chemicals

Figure 3.8 Mr. Jeremiah of Deforest Wood Preserving boring cores from lumber in charge to test for preservative retention

Figure 3.9 CLT panels under breezeway of Franklin Center at Mississippi State University

3.3.4 Block shear test method

Specimens were air dried following treatment. The approximate moisture content of the CLT panels was 20% as measured with a TackLife Model MWM02 handheld wood moisture tester after 4 months of air drying. Each CLT panel was cut into 15 square blocks measuring 133 mm x 133 mm x 104 mm for 3-ply panels and 133 x 133 mm x 175 mm for 5-ply panels (Figures 3.10 and 3.11).

Figure 3.10 Cutting CLT panels into square blocks

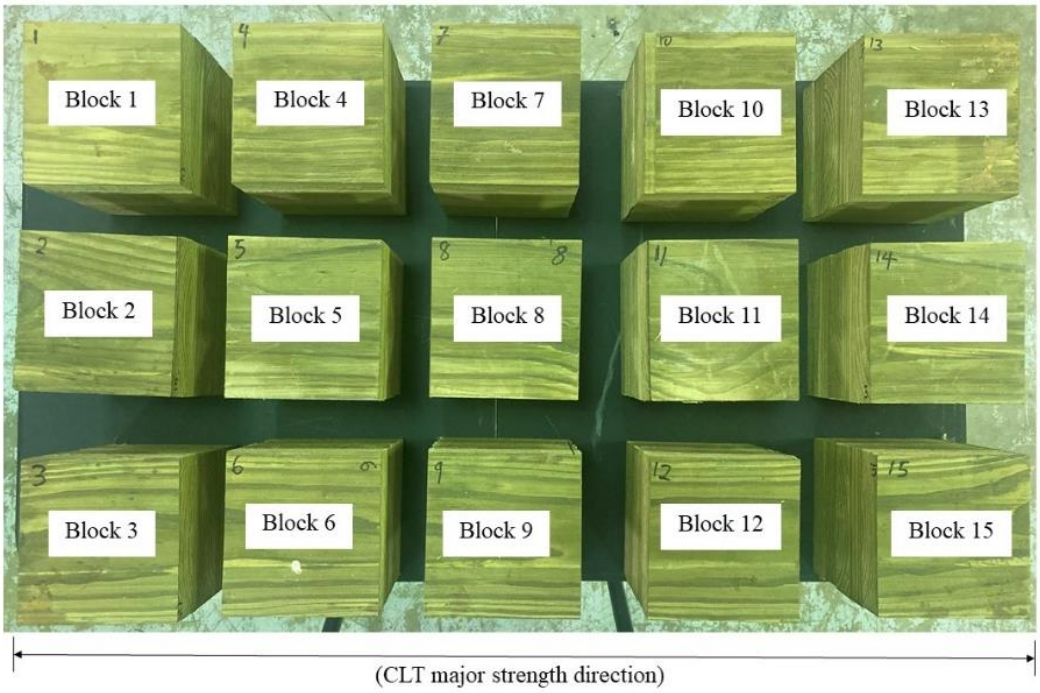

Figure 3.11 One CLT panel cut into 15 square blocks

Shear block specimens were prepared by referencing ASTM D2559 (2017). For each panel configuration shear block specimens and delamination, specimens were cut from five different locations (1,2,7,8,15) (Figure 3.11). Blocks 1 and 15 represents corner positions. Blocks 2 and 7 represent end positions and Block 8 represents the middle of the panel. The shear block specimens for Configurations 1 and 2 were cut to 63.5 mm x 50.8 mm (Figure 3.12a). The shear block specimens for Configuration 3 were cut to 114.3 mm x 50.8 mm (Figure 3.12b). The shear block specimens were stair-stepped with a shearing area of 50.8 mm x 38.1 mm. The shear block specimens were conditioned at 21°C and 65% RH for at least 5 months.

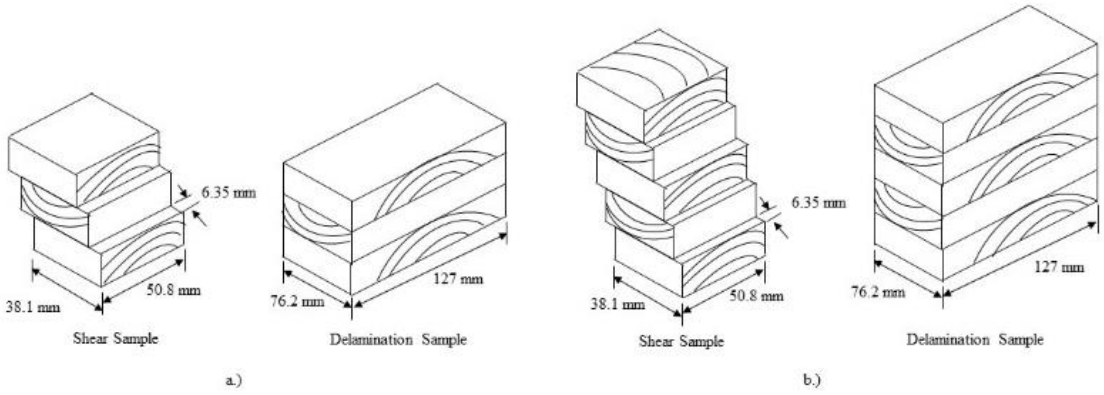

Figure 3.12 a.) 3-ply CLT shear and delamination sample b.) 5-ply CLT shear and delamination sample

The tests were carried out per ASTM D905 (2021). Figure 3.13 shows the test setup. The shearing tool applied a force through adjacent laminations at a rate of 5.08 mm/min until failure. Images of the failure shear plane were scanned using a Canon CanoScan LiDe 400 scanner which has a maximum optical resolution of 4800 x 4800 dpi. The shear plane was analyzed using ImageJ2, an image processing software. Block shear strength (BSS) (f_v) was calculated as:

$$fv = \mathrm{Fu/A} \tag{3.1}$$

where Fu = failure load (N) and A is the sheared area (mm^2). The percentage of wood failure (WFP) on the shear block failure plane was also measured using ImageJ2 software (Rueden 2017). The shear blocks were analyzed for the modes of failure: adhesive failure (AD), failure parallel-to-grain (PAR), and failure perpendicular-to-grain (PER, rolling shear). The WFP was measured by dividing the wood failure area by the tested shear bonded area. The WFP was estimated per ASTM D5266 (2005).

Figure 3.13 Block shear specimen in block shear set-up in Tinius Olsen Machine

3.3.5 Delamination test method

Delamination specimens were prepared by referencing ASTM D2559 (2017). For each panel configuration delamination specimens were cut from five different locations (1,2,7,8,15) (Figure 3.11). The delamination specimens were cut to 127 mm x 76.2 mm for all three

configurations (Figures 3.12a and 3.12b). The delamination specimens were conditioned at 21°C and 65% RH for at least 5 months. Three sides of each specimen were digitized using a Canon CanoScan LiDE 400 scanner which has a maximum optical resolution of 4800 x 4800 dpi. Figure 3.14 shows the equipment used for conducting the delamination test. Figure 3.15 outlines the delamination test procedure.

The delamination specimens were weighed to the nearest 1 gram before testing. The specimens were placed in the wire mesh basket (Figure 3.14c). The wire mesh basket was then placed in the pressure vessel (Figure 3.14a). The pressure vessel was sealed and filled with water at a temperature of 21°C and placed under vacuum for 5 minutes at 30 psi (0.207 MPa). After the vacuum was released, the specimens were placed under air pressure for 1 hour at 75 psi (0.517 MPa). The vacuum-pressure cycle was repeated, the specimens had to increase in weight by at least 50%. The specimens were removed from the pressure vessel and placed in the oven at 65°C for approximately 22 hours with the test bond lines parallel to the air flow in the oven (Figure 3.16). The specimens were dried to within 15% of their original weights. The specimens were placed back into the wire mesh basket and placed back in the pressure vessel and sealed to be subjected to steam at 100°C for 90 minutes. The pressure vessel was cooled by flushing with tap water at 21°C until the temperature thermocouple on the pressure vessel displayed ambient temperature. The pressure vessel was then filled with water and placed under air pressure for 40 minutes at 75 psi (0.517 MPa). The specimens were removed from the pressure vessel and placed back in the drying oven at 65°C as described above. After returning to within 15% of their original weight, the specimens were placed back in the pressure vessel for a repeat of Day 1 vacuum-pressure cycles. The specimens were removed from the pressure vessel and placed back in the drying oven at 65°C. After drying to within 15% of the original weight, the delamination

was measured along the test bond lines, and recorded. Three sides of each specimen were digitized with the scanner as before. A feeler gauge of 0.08 mm was also used to determine separations in the glue line.

a) b) c)

Figure 3.14 Delamination test equipment: a) pressure vessel; b) blue m oven; c) samples in wire mesh basket

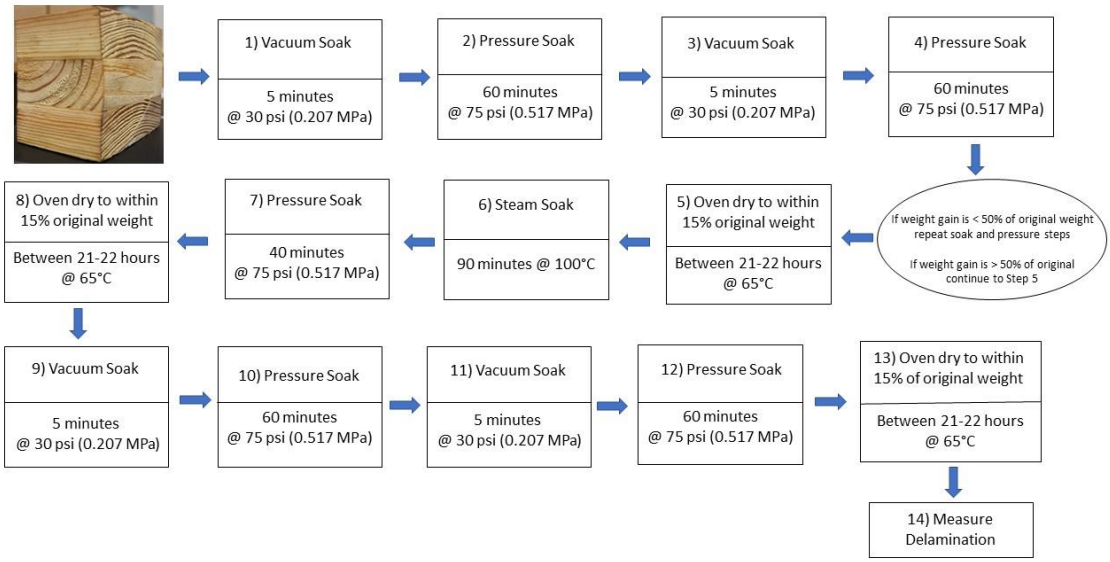

Figure 3.15 Outline of test procedure for delamination testing based on ASTM D2559

Figure 3.16 Oven-dry process for delamination test

The total delamination Delamtot of a test piece was calculated as:

$$\text{Delamtot} = 100\ (\text{ltot, delam})/(\text{ltot, glue line})\ \text{in}\ \% \qquad (3.2)$$

where ltot,delam = the total delamination length and ltot, glue = the sum of the glue lines for five specimens in a panel.

Figure 3.17 shows the bondlines of the delamination samples which were labeled across the length (labeled “A” and “B” for 3-ply, labeled “A”, ”B”, “C”, and “D” for 5-ply). Delamination was measured immediately after the specimens underwent cycles of vacuum, soaking, and oven-drying procedures as specified in ASTM D 2559.

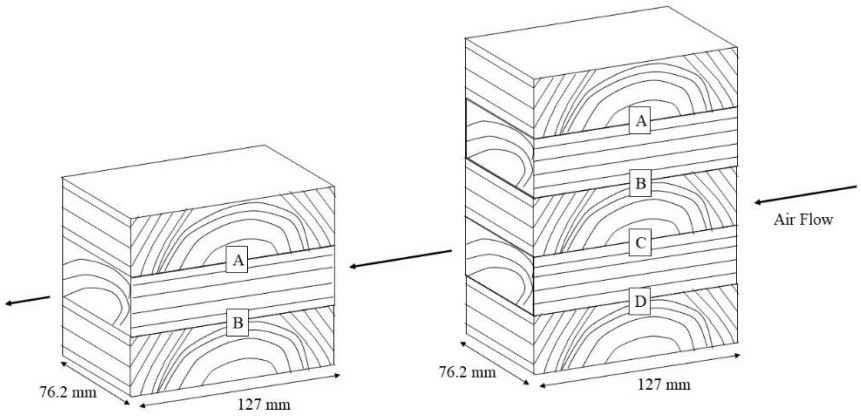

Figure 3.17 Orientation of the delamination test specimen during the oven-drying procedure. A and B denote two bond lines for 3-ply CLT. A, B, C, D denote four bond lines for 5-ply CLT.

3.3.6 Statistical Analysis

The effects of panel layup (lengthwise and crosswise) and thickness (3-ply and 5-ply) on the bonding performance (block shear strength and wood failure percentage) and durability (delamination) was studied in post treated CLT panels. The data was analyzed using SAS version 9.4. The assumption of normality and homogeneity of variance were tested on the raw data using

the Shapiro-Wilk test and Levene's test, respectively. If the assumptions were not meet, the data was transformed by logarithmic-transformation, i.e. log(x), and tested again for normality and homogeneity of variance. If the data could not be normalized, the Kruskal-Wallis H test, a non-parametric equivalent of ANOVA was used to analyze the significance of the main effects. If the main effects proved to be significant at $\alpha = 0.05$, then mean rank separation was done using Dunn's pairwise test adjusted by the Bonferroni correction. If assumptions of normality and homogeneity of variance were satisfied ($p > 0.05$), a one-way ANOVA and the Tukey Honestly Significant Difference (HSD) test was performed for mean separation within the main effects.

3.4 Results and Discussion

3.4.1 Panel Air Drying

Before treating, the MC% of all the CLT panels was approximately 12%, which is within the target moisture content range for the adhesive specifications. The average moisture content (MC%) of the panels after returning from the treaters was over 85% (Figures 3.18 to 3.23). The average equilibrium moisture content (EMC) conditions to which the panels were subjected at Franklin Center at Mississippi State University was approximately 17% (measured from 03/28/2021 - 07/30/2021). After treatment, the air-dried MC% of the treated CLT panels for both MCA and CA-C after 4 months was 25%, which was close to the estimated target of 20%. While the MC% of untreated panels remained 12%, these panels were placed outdoors under a protected roof along with the treated CLT panels in order to moisture equilibrated at approximately 18%.

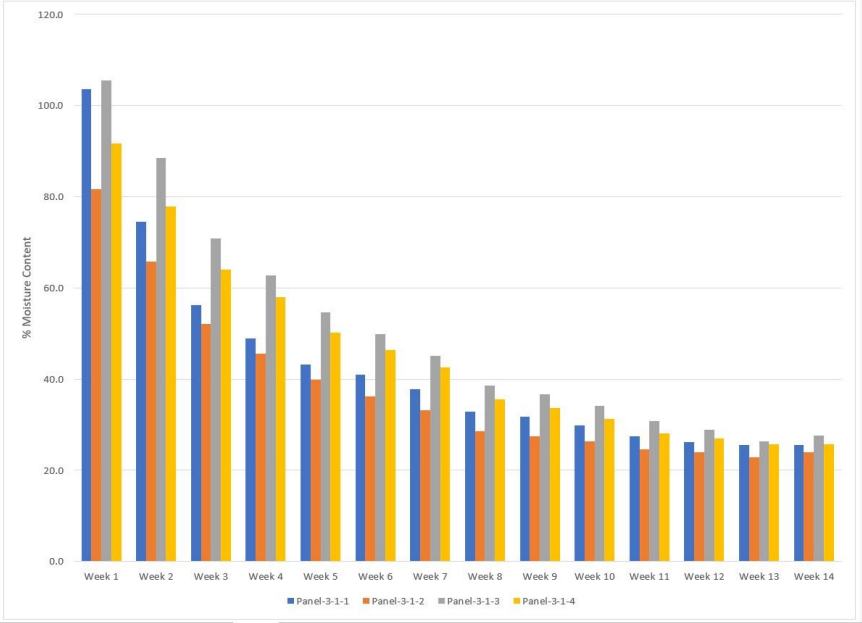

Figure 3.18 Moisture contents of CA-C panels from Configuration 1

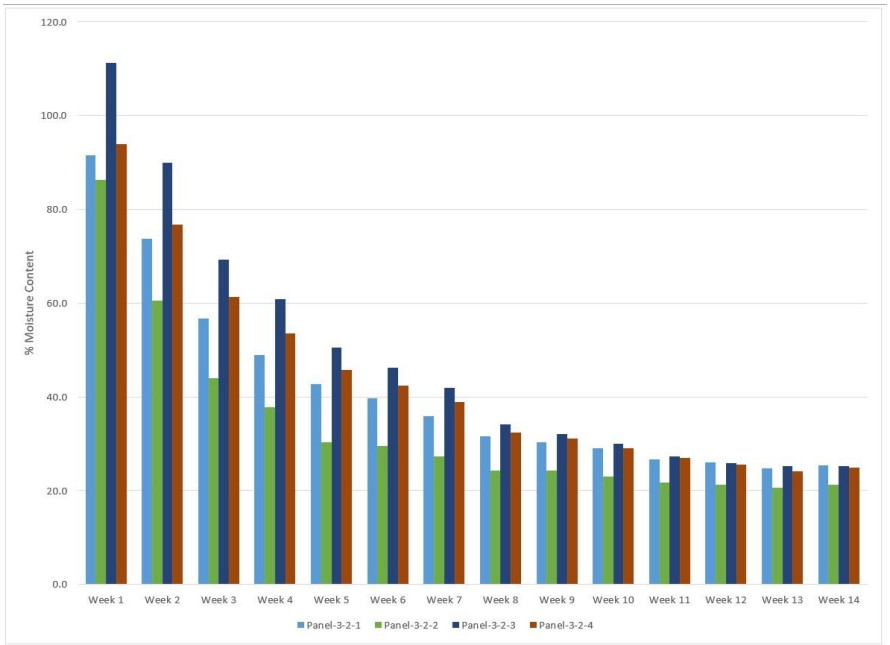

Figure 3.19 Moisture contents of CA-C panels from Configuration 2

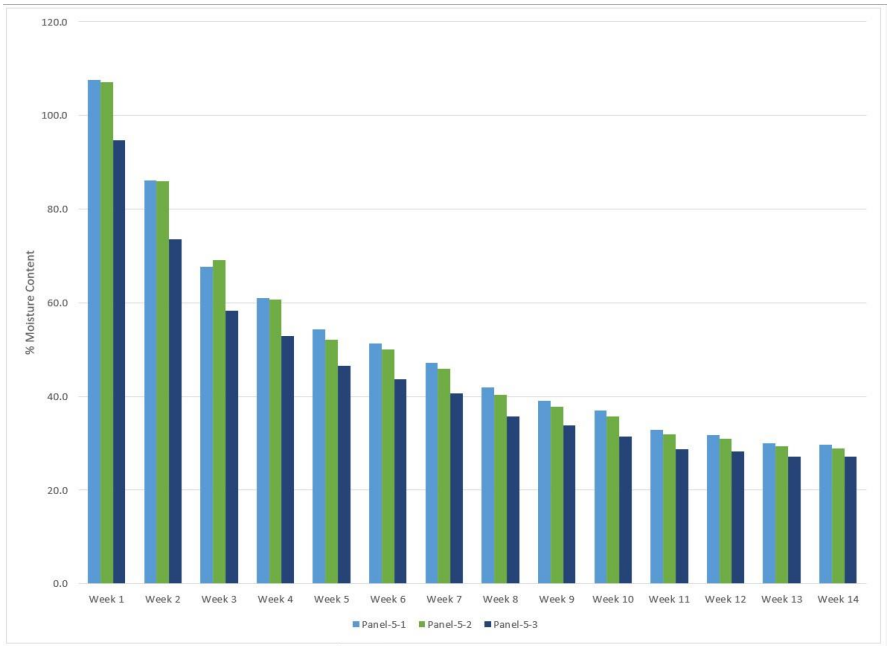

Figure 3.20 Moisture contents of CA-C panels from Configuration 3

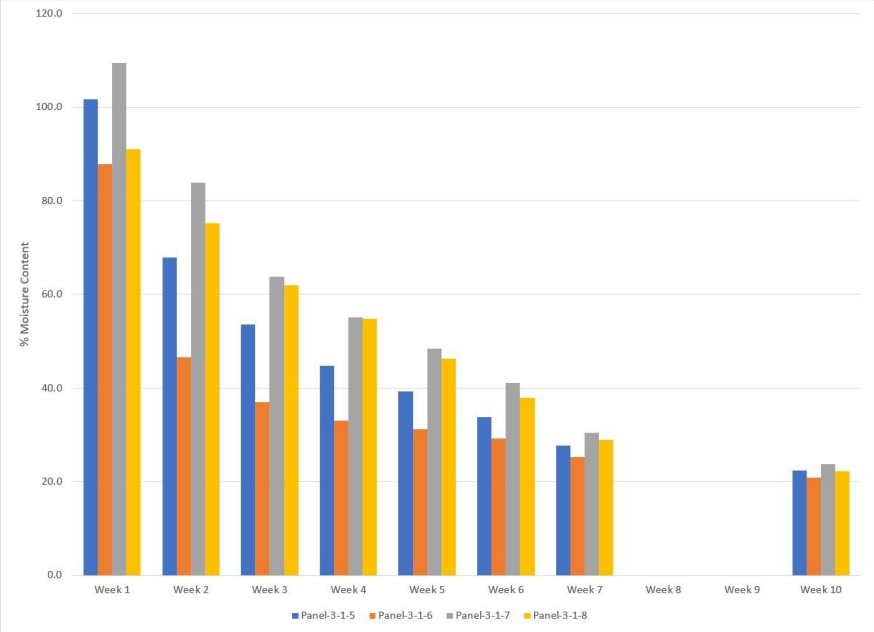

Figure 3.21 Moisture contents of MCA panels from Configuration 1

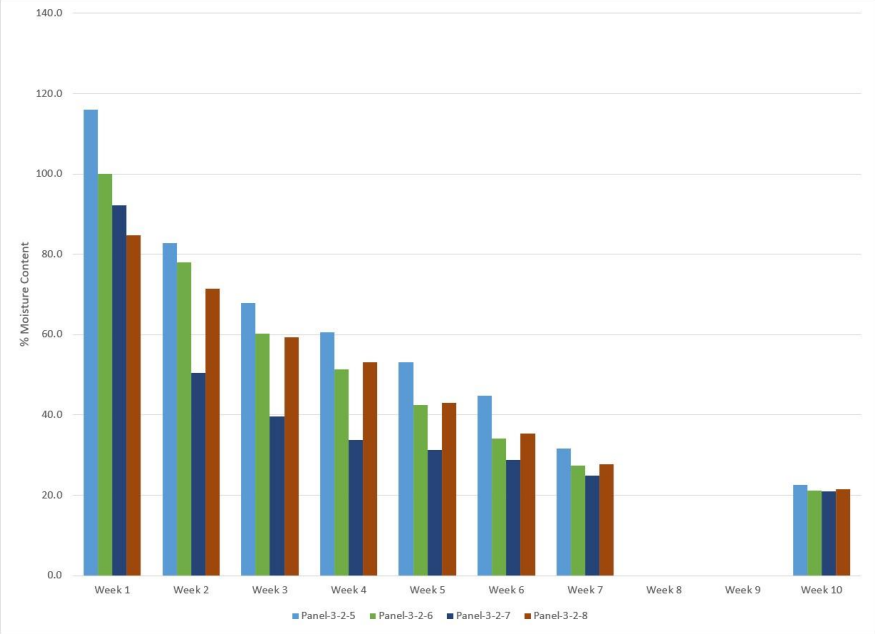

Figure 3.22 Moisture contents of MCA panels for Configuration 2

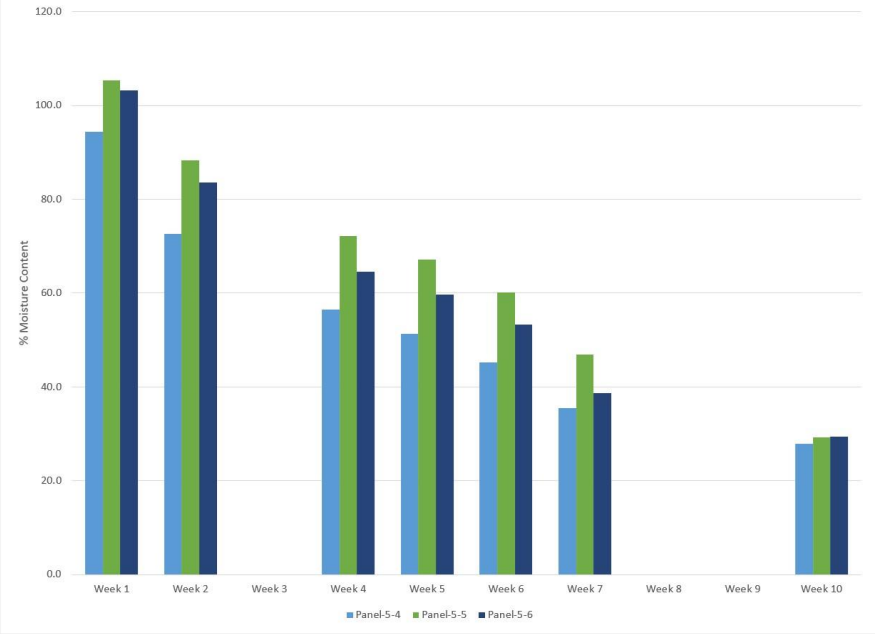

Figure 3.23 Moisture contents of MCA panels for Configuration 3

3.4.2 Block Shear Test

The descriptive statistics for the calculated BSS and WFP for the nine CLT groups are shown in Table 3.3. Even though the block shear test was conducted by referencing ASTM D 2559, the BSS values were not compared to a standard requirement. As an example, structural glued laminated timber has a standard requirement. The minimum BSS value in the standard is 8.6 MPa which is the average parallel-to-grain shear strength of SYP at 12% moisture content. Because the average shear strength of wood is less perpendicular-to-grain, the major governing failure mode for CLT shear blocks was shear perpendicular-to-grain (rolling shear). The average BSS of the control samples ranged from 3.13 MPa to 4.44 MPa with COVs ranging from 20.27% to 34.79%. The CA-C and MCA treatments measured lower BSS values than the control groups for Configuration 1 and Configuration 3. For Configuration 2 the CA-C treatment group developed a higher BSS value than the control group. The only groups to pass the minimum average 75% WFP required by ASTM D2559 were Configuration 1 control group, Configuration 1 CA-C treated group, Configuration 2 control group, Configuration 3 CA-C treated group, and Configuration 3 MCA treated group. 129 out of 300 block shear tests had a WFP < 75%. Approximately 60% of the block shear specimens passed the minimum WFP requirement of 75% per ASTM D2559. Of those 129 block shear specimens that fell short of 75% WFP (Table 3.3), most of the specimens were close to meeting the minimum WFP requirements (88 had WFP between 50 and 75%). The boxplots of the BSS and WFP are presented in Figures 3.24 and 3.25, respectively.

Table 3.3 Descriptive statistics of BSS (block shear strength) and WFP (wood failure percentage) for the nine CLT groups.

CLT Group*	Sample Size	BSS(MPa) Mean [95% CI**]	BSS(MPa) Median [range]	BSS(MPa) COV (%)	WFP(%) Mean	WFP(%) Median [range]	No.<75% WFP***
1C	20	4.44 [3.95-4.93]	4.31 [3.03-7.52]	25.64	78.75	85.00 [20.00-100.00]	8
1CAC	40	3.26 [2.83-3.69]	3.27 [0.37-5.10]	30.45	79.13	80.00 [30.00-100.00]	13
1MCA	40	2.94 [2.54-3.34]	2.90 [0.62-4.60]	30.79	74.00	77.50 [5.00-100.00]	17
2C	20	3.08 [2.81-3.35]	2.84 [2.17-4.73]	20.27	85.00	100.00 [30.00-100.00]	5
2CAC	40	3.32 [3.04-3.72]	3.15 [1.96-6.36]	22.76	66.00	65.00 [15.00-100.00]	28
2MCA	40	2.93 [2.44-3.42]	3.02 [0.10-5.64]	37.76	70.25	72.50 [5.00-100.00]	20
3C	20	3.13 [2.65-3.61]	3.42 [0.53-5.52]	34.79	68.75	70.00 [0.00-100.00]	11
3CAC	40	2.78 [2.52-3.04]	2.81 [1.44-4.05]	21.18	81.00	80.00 [45.00-100.00]	13
3MCA	40	3.01 [2.69-3.33]	2.93 [1.90-4.76]	24.53	81.37	95.00 [30.00-100.00]	14

*CLT Group, 1C (Configuration-1 Control), 1CAC (Configuration-1 CA-C), 1MCA (Configuration-1 MCA), 2C (Configuration-2 Control), 2CAC (Configuration-2 CA-C), 2MCA (Configuration-2 MCA), 3C (Configuration-3 Control), 3CAC (Configuration-3 CA-C), 3MCA (Configuration-3 MCA)

**CI, confidence interval

***Number of specimens with < 75% WFP

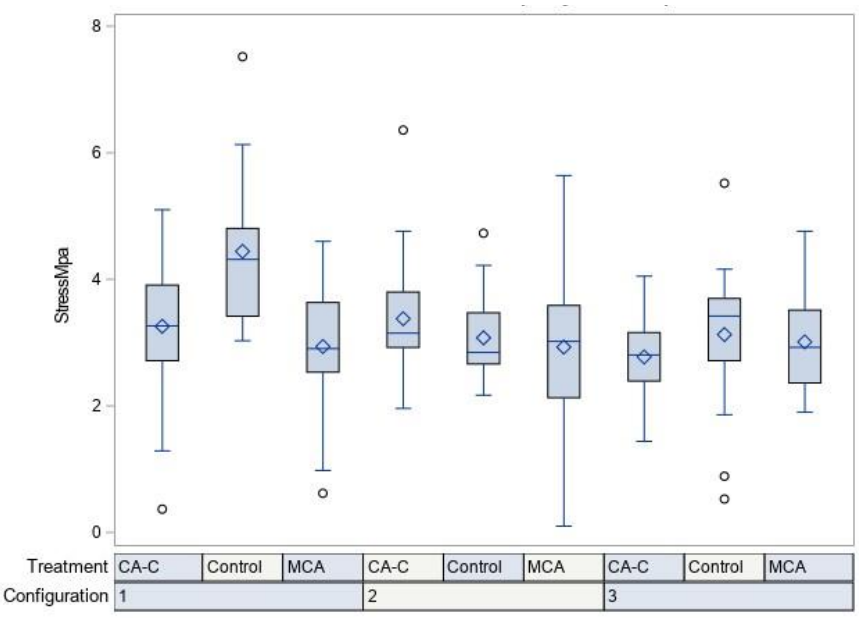

Figure 3.24 Boxplots of BSS (Block Shear Strength). Boxplots: circles indicate outliers; diamonds indicate mean values; colored boxes indicate lower quartile; upper and lower bars indicate minimum and maximum values

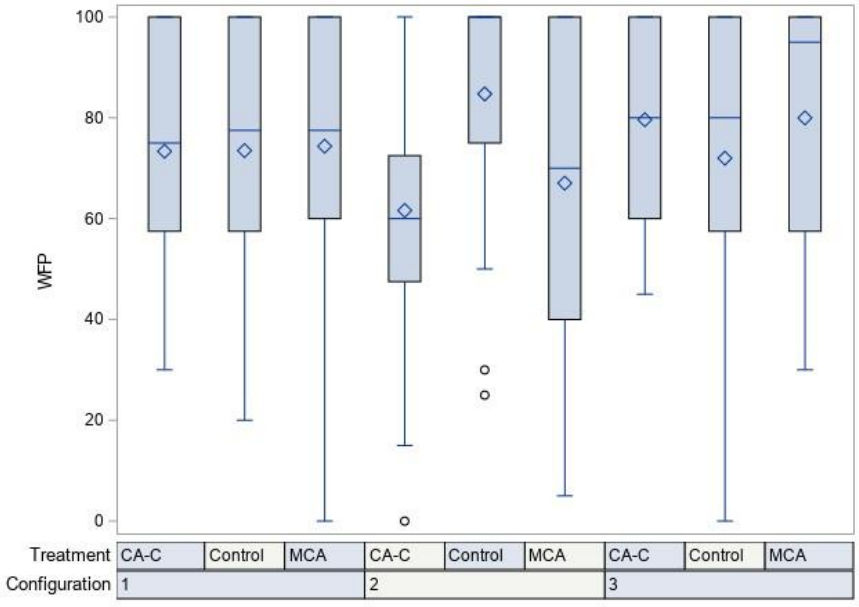

Figure 3.25 Boxplots of WFP (Wood Failure Percentage). Boxplots: circles indicate outliers; diamonds indicate mean values; colored boxes indicate lower quartile; upper and lower bars indicate minimum and maximum values

3.4.2.1 Effect of preservative treatment

For the 3-ply parallel configurations, a one-way ANOVA was used to compare the effects of preservative treatment on mean BSS values since the datasets passed the normality and equality of variance tests. For the 3-ply cross configurations and the 5-ply parallel configurations, the datasets passed the normality tests, but failed to pass the equality of variance tests, therefore the mean BSS ranks were tested using the Kruskal-Wallis H test. The only configuration group that was influenced by preservative treatment was the 3-ply parallel configuration. The mean BSS value for the untreated controls were statistically higher than the mean BSS values for the CA-C and MCA treatments (Figure 3.26). Studies have shown that the BSS of preservative treated wood could be lower than untreated wood, but this is when the laminates were bonded post treatment. The specimens herein were bonded and then treated after the gluing process. There was statistically no significant difference between the treatments within the 3-ply cross and the 5-ply parallel configurations.

To compare the effects of preservative treatment on the WFP, the Kruskal-Wallis H test was used because all the datasets failed to pass the normality and the equality of variance tests. The 3-ply cross configuration showed that the preservative treatment influenced WFP with the untreated control samples measuring a significantly higher percentage of wood failure at 85% with the CA-C and MCA treatments measuring a wood failure of approximately 70%. The WFP for the 3-ply parallel and the 5-ply parallel was not influenced by the preservative treatment measuring a percentage wood failure between 70% and 80% (Figure 3.27).

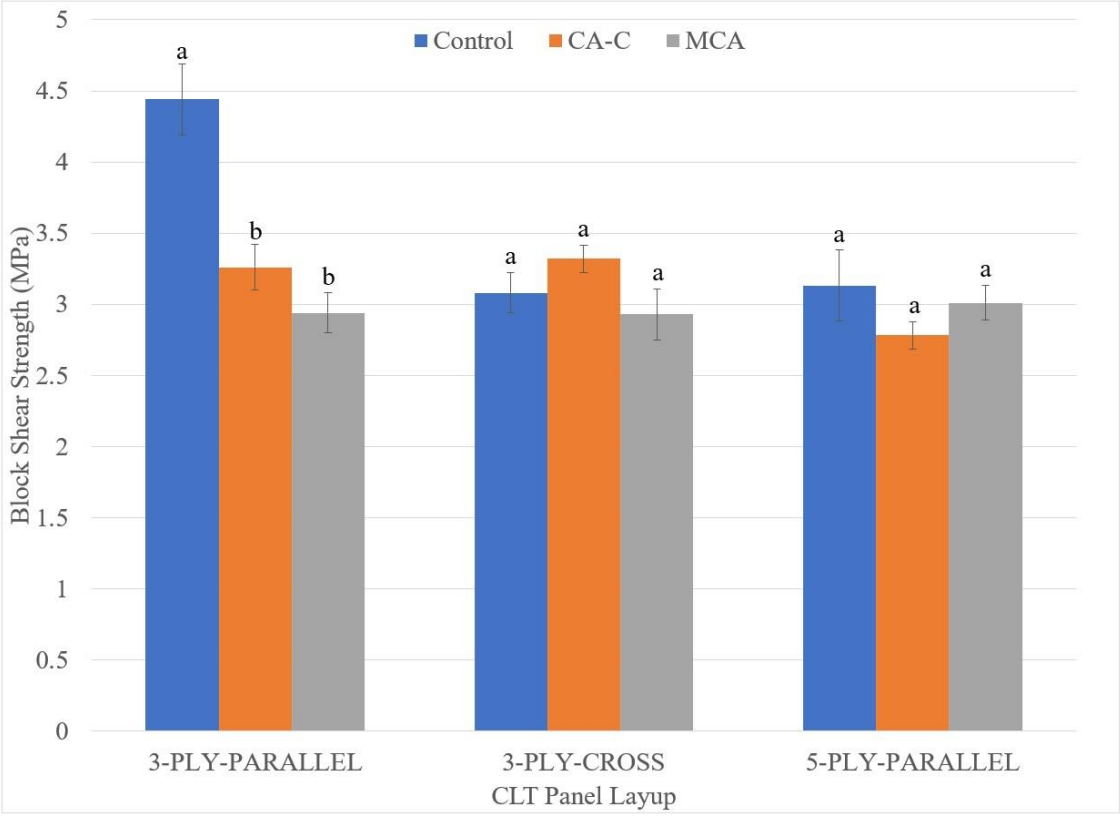

Figure 3.26 Mean BSS of the CLT treatment by panel layup (bars represent standard error; different letters above the bars indicate significant differences ($p<0.05$) among the treatment means for within panel layup; for pairwise comparisons, Tukey HSD was used for 3-ply parallel configuration while Dunn's test with p-values adjusted by the Bonferroni correction was used for 3-ply cross and 5-ply parallel configurations)

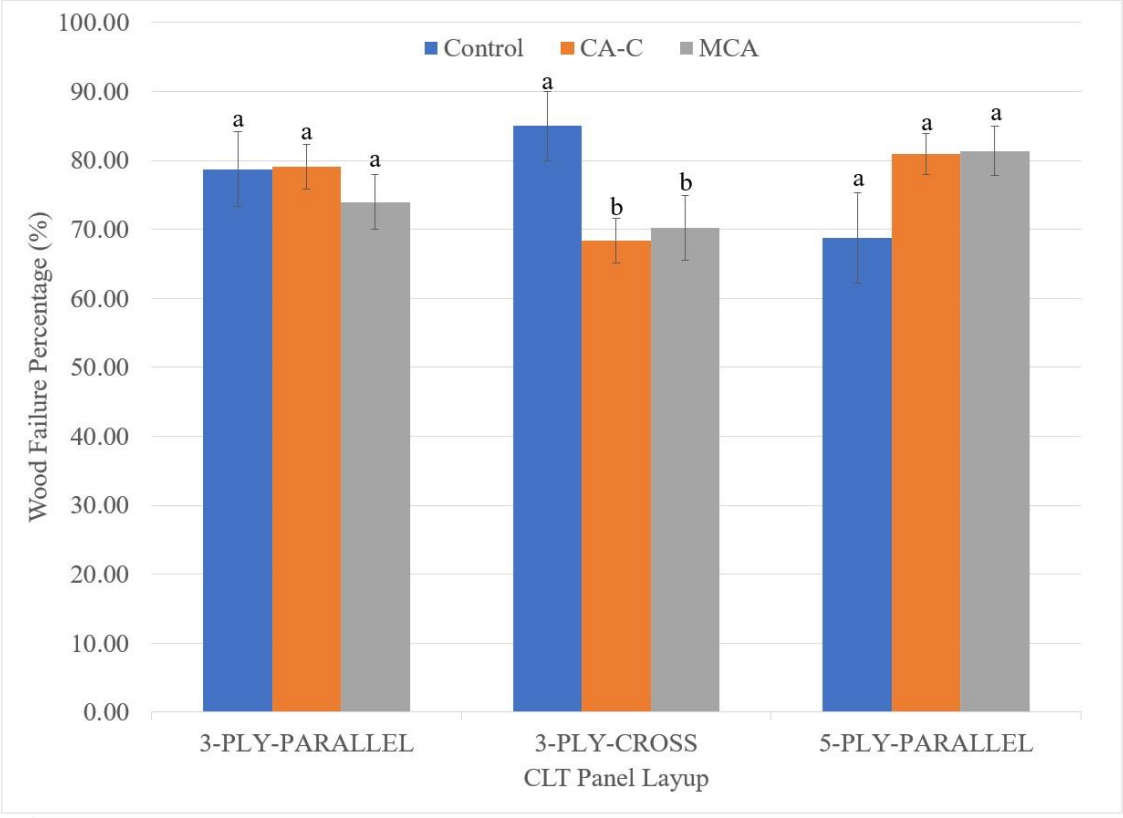

Figure 3.27 Mean WFP of CLT treatment by panel layup (bars represent standard error, different letters above the bars indicate significant differences ($p<0.05$) among the treatment means for within panel layup; for pairwise comparisons Dunn's test with p-values adjusted by the Bonferroni correction was used for all three configurations)

3.4.2.2 Effect of panel layup and thickness

For the untreated control samples and the MCA treated samples, a one-way ANOVA was used to compare the effects of panel layup on mean BSS values since the datasets passed the normality and equality of variance tests. For the CA-C treated samples, the dataset passed the normality tests, but failed to pass the equality of variance tests, therefore the mean BSS ranks was tested using the Kruskal-Wallis H test. The control samples and the CA-C samples were influenced by the layup of the panels. For the control samples the 3-ply parallel samples measured a significantly higher mean BSS than the 3-ply cross and the 5-ply parallel. The 5-ply

parallel samples measured a significantly lower mean BSS than the 3-ply parallel and 3-ply cross samples. The mean BSS of the MCA samples were not significantly influenced by the panel layup (Figure 3.28).

The WFP of the CA-C samples were the only ones influenced by the layup of the panels. The 3-ply cross panels measured a significantly less WFP than the 3-ply parallel and the 5-ply parallel. The WFP for the control and the MCA samples were not significantly influenced by the panel layup (Figure 3.29).

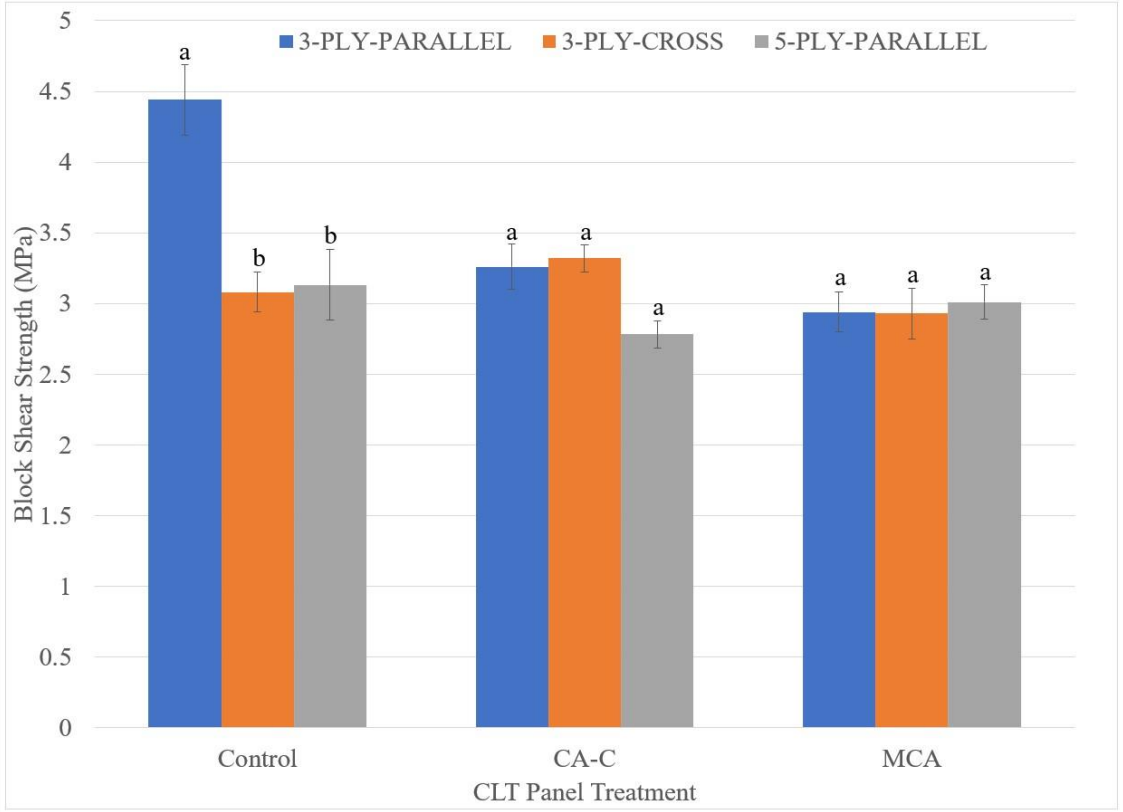

Figure 3.28 Mean BSS of CLT panel layup and thickness by preservative treatment (bars represent standard error; different letters above the bars indicate significant differences ($p<0.05$) among the panel layup and thickness within treatments; for pairwise comparisons, Tukey HSD was used for untreated controls and the MCA treatment while Dunn's test with p-values adjusted by the Bonferroni correction was used for CA-C treatment)

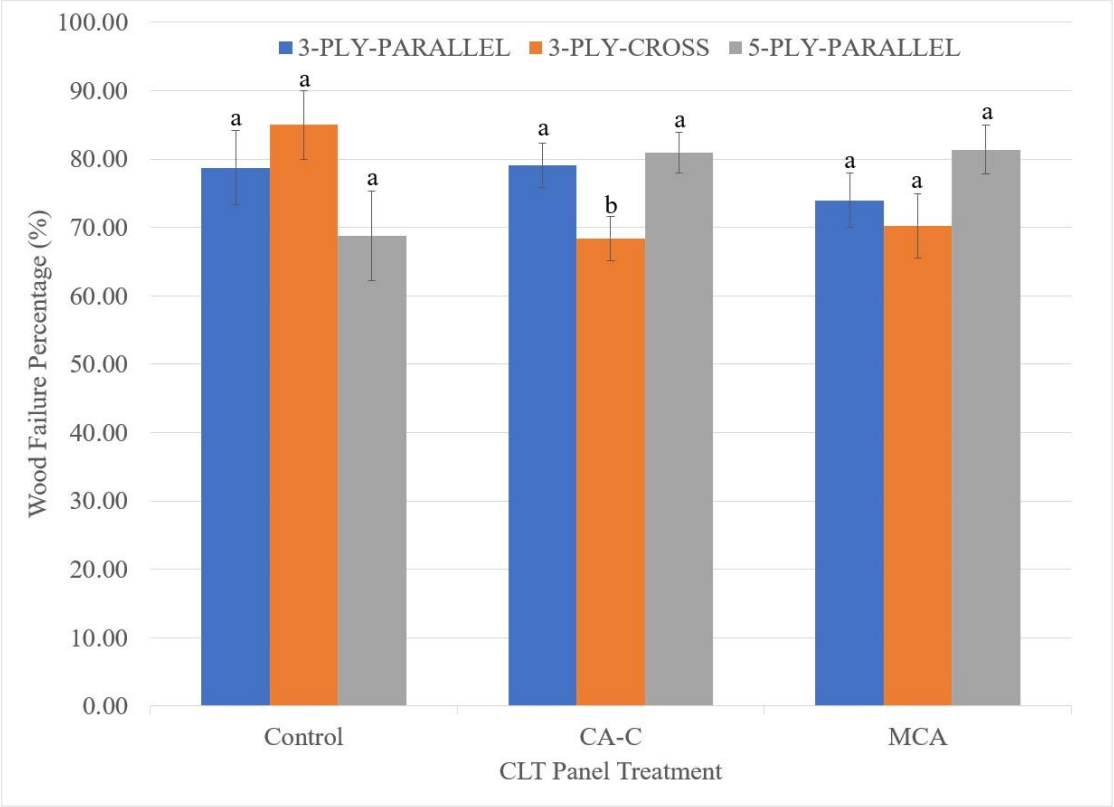

Figure 3.29 Mean WFP of CLT panel layup and thickness by preservative treatment (bars represent standard error, different letters above the bars indicate significant differences ($p<0.05$) among the panel layup within treatments; for pairwise comparisons, Dunn's test with p-values adjusted by the Bonferroni correction for all three treatments

3.4.2.3 Failure modes

The three failure modes recognized for the block shear tests are shown in Figure 3.30. AD (adhesive failure) occurred when the adhesive failed when the adhesive bond was weaker than the wood. PER (perpendicular-to-grain (rolling shear)) and PAR (parallel-to-grain) occurred when the adhesive bond was stronger than the wood. Most of the specimens (at least 50%) had PER failure because the shear strength of wood is significantly less perpendicular to the grain as compared to parallel to the grain. The untreated control groups had the smallest percentage of

adhesive failure as the controlling failure mode. Table 3.4 list a breakdown of the observed controlling failure modes for each specimen.

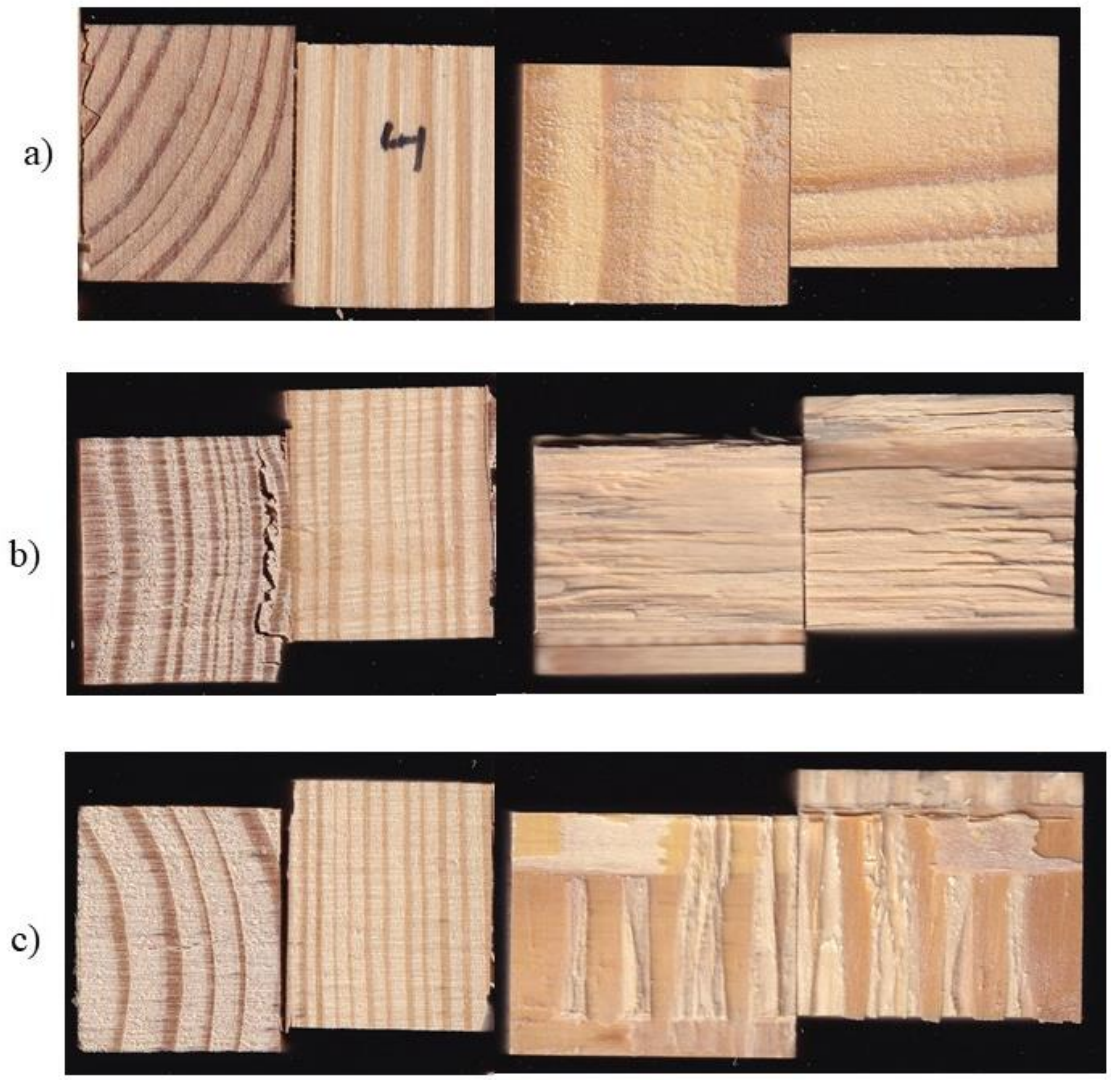

Figure 3.30 Failure modes of block shear specimens: a) AD – adhesive failure, b) PER – perpendicular-to-grain (rolling shear), c) PAR – parallel-to-grain

Table 3.4 Block shear test results by controlling failure mode.

CLT Group*	Number of observations (mean BSS in MPa)				
	AD	PAR	PER	PAR/PER	Total
1C	3	4	13	0	20
	(4.90)	(4.64)	(4.27)	(N/A)	(4.44)
1CAC	6	9	24	1	40
	(3.46)	(3.45)	(3.06)	(5.10)	(3.26)
1MCA	12	4	24	0	40
	(2.72)	(3.33)	(2.99)	(N/A)	(2.94)
2C	3	0	17	0	20
	(2.85)	(N/A)	(3.12)	(N/A)	(3.08)
2CAC	10	6	24	0	40
	(3.45)	(3.56)	(3.21)	(N/A)	(3.38)
2MCA	13	7	19	0	40
	(3.11)	(3.01)	(2.79)	(N/A)	(2.93)
3C	5	1	12	2	20
	(2.11)	(2.63)	(3.65)	(2.77)	(3.13)
3CAC	6	5	29	0	40
	(2.83)	(2.84)	(2.75)	(N/A)	(2.78)
3MCA	10	6	22	2	40
	(3.24)	(3.38)	(2.76)	(3.54)	(3.01)

*CLT Group, 1C (Configuration-1 Control), 1CAC (Configuration-1 CA-C), 1MCA (Configuration-1 MCA), 2C (Configuration-2 Control), 2CAC (Configuration-2 CA-C), 2MCA (Configuration-2 MCA), 3C (Configuration-3 Control), 3CAC (Configuration-3 CA-C), 3MCA (Configuration-3 MCA)
AD – adhesive failure; PAR – parallel-to-grain wood failure; PER – perpendicular-to-grain wood failure; BSS – block shear strength

3.4.3 Delamination Test

Table 3.5 shows the results of the delamination test. The delamination rates ranged from 2.0% (5-ply parallel Glue Line B) to 25.8% (3-ply cross Glue Line A). The only glue lines that passed the ASTM D2559 allowable delamination of 1% for softwoods was the 5-ply parallel Glue Lines C and D. The untreated control specimens measured the smallest average delamination rate. The CA-C treated specimens measured a smaller delamination rate as compared to the MCA treated specimens. On average the preservative treatment, panel layup and panel thickness all had an influence on the delamination rate. Figure 3.31 presents the modes of

failure observed during the delamination test. In-plane and out-of-plane changes in dimension caused by shrinking and swelling of the laminates were the governing modes of failure.

Table 3.5 Summary of delamination test results.

CLT Group [A]	Bondline	Bondline Delamination, (mm)[B]	Bondline Length (mm)[C]	Delamination Rate (%)[D]
1C	A	219.1	2540	8.6
	B	139.7	2540	5.5
1CAC	A	727.1	5080	14.3
	B	266.7	5080	5.3
1MCA	A	974.7	5080	19.2
	B	995.4	5080	19.6
2C	A	654.1	2540	25.8
	B	301.6	2540	11.9
2CAC	A	871.5	5080	17.2
	B	808.0	5080	15.9
2MCA	A	800.1	5080	15.8
	B	1162.1	5080	22.9
3C	A	74.6	1270	5.9
	B	25.4	1270	2.0
	C	0	1270	0
	D	0	1270	0
3CAC	A	509.6	2540	20.1
	B	303.2	2540	11.9
	C	195.3	2540	7.7
	D	388.9	2540	15.3
3MCA	A	376.2	2540	14.8
	B	331.8	2540	13.1
	C	290.5	2540	11.4
	D	134.9	2540	5.3

[A]CLT Group, 1C (Configuration-1 Control), 1CAC (Configuration-1 CA-C), 1MCA (Configuration-1 MCA), 2C (Configuration-2 Control), 2CAC (Configuration-2 CA-C), 2MCA (Configuration-2 MCA), 3C (Configuration-3 Control), 3CAC (Configuration-3 CA-C), 3MCA (Configuration-3 MCA)

[B]Sum of delamination length on two sides of all specimens for each bond line; [C]Sum of bond line length on two sides of all specimens for each bond line; [D]Bond line delamination divided by total bond line multiplied by 100

Figure 3.31 Wood laminates after accelerated weather cycles: a) dimensional changes out of plane and b) dimensional changes in-plane

3.5 Conclusion

The effect of the MCA and CA-C treatment and CLT panel layup on the bonding performance of post treated SYP CLT panels manufactured using a one component PUR adhesive was investigated by conducting block shear and delamination tests. The only configuration group for BSS that was influenced by preservative treatment was the 3-ply parallel configuration. There was statistically no significant difference between the treatments within the 3-ply cross and the 5-ply parallel configurations for BSS. The mean WFP was over 70% for all the configurations except for the 3-ply cross configuration and the 5-ply parallel configuration. The panel layup influenced the BSS with the 5-ply parallel configuration measuring the lower BSS. The perpendicular to grain was the major failure mode observed for the block shear samples. Most of the specimens had large percentages of delamination except for the control groups. The 3-ply cross control had a higher delamination rate which could not be explained.

3.6 References

Adan NA, Tahir P, Husain H, Lee SH, Uyup MKA, Arip MNM, and Ashaari Z. 2021. Effect of ACQ Treatment on Surface Quality and Bonding Performance of Four Malaysian Hardwoods and Cross Laminated Timber (CLT). European Journal of Wood and Wood Products 79:285-299.

American Society for Testing and Materials. 2005. D 5266. Standard Practice for Estimating the Percentage of Wood Failure in Adhesive Bonded Joints. ASTM International. West Conshohocken, PA.

American Society for Testing and Materials. 2017. D 2395. Standard Test Methods for Density and Specific Gravity (Relative Density) of Wood and Wood-Based Materials. ASTM International. West Conshohocken, PA.

American Society for Testing and Materials. 2018. D 2559. Standard Specification for Adhesives for Bonded Structural Wood Products for Use Under Exterior Exposure Conditions. ASTM International. West Conshohocken, PA.

American Society for Testing and Materials. 2020. D 4442. Standard Test Methods for Direct Moisture Content Measurement of Wood and Wood-Based Materials. ASTM International. West Conshohocken, PA.

American Society for Testing and Materials. 2021. D 905. Standard Test Method for Strength Properties of Adhesive Bonds in Shear by Compression Loading. ASTM International. West Conshohocken, PA.

ANSI/APA. 2018. Standard for Performance-Rated Cross Laminated Timber. ANSI/APA PRG 320. Tacoma, Washington, USA.

AWPA P48-15. 2017. Standard for Copper Azole Type C (CA-C). American Wood Protection Association. Birmingham, AL.

AWPA P61-16. 2017. Standard for Micronized Copper Azole (MCA). American Wood Protection Association. Birmingham, AL.

Brandner R, Flatshcer G, Ringhofer A, Schickhofer G, and Thiel A. 2016. Cross Laminated Timber (CLT): Overview and Development. European Journal of Wood and Wood Products 74:331-351.

Freeman M and McIntyre C. 2008. A Comprehensive Review of Copper-Based Wood Preservatives. Forest Products Journal 58(11):6-27.

Gagnon S and Pirvu C. 2011. CLT Handbook-Canadian Edition. FP Innovations, Quebec, Canada.

De Groot R and Woodward B. 1999. Using Copper-Tolerant Fungi to Biodegrade Wood Treated with Copper-Based Preservatives. International Biodeterioration and Biodegradation 44(1):17-27.

Lee D, Lee MJ, Son D, and Park BD. 2006. Adhesive Performance of Woods Treated with Alternative Preservatives. Wood Science Technology 40:228-236.

Lim H, Tripathi S, and Tang J. 2020. Bonding Performance of Adhesive Systems for Cross-Laminated Timber Treated with Micronized Copper Azole Type C (MCA-C). Construction and Building Materials 232:1-10.

Lisperguer JH and Becker PH. 2005. Strength and Durability of Phenol-Resorcinol-Formaldehyde Bonds to CCA-Treated Radiata Pine Wood. Forest Products Journal 55(12):113-116.

Muszynski L, Hansen E, Fernando S, Schwarzmann G, and Rainer J. 2017. Insights into the Global Cross-Laminated Timber Industry. BioProducts Business 2(8):77-92.

Nguyen T, Li J, and Li S. 2012. Effects of Water-Borne Rosin on the Fixation and Decay Resistance of Copper-Based Preservative Treated Wood. BioResources 7(3):3573-3584.

Pierobon F, Huang M, Simonen K, and Ganguly I. 2019. Environmental Benefits of using Hybrid CLT Structure in Midrise Non-Residential Construction: An LCA Based Comparative Case Study in the U.S. Pacific Northwest. Journal of Building Engineering 26(11):1-14.

Rueden CT, Schindelin J, Hiner MC, DeZonia BE, Walter AE, Arena ET, and Eliceiri KW. 2017. Image J2: ImageJ for the Next Generation of Scientific Image Data. BMC Bioinformatics 18:529.

SAS Institute. 2016. SAS Software, Version 9.4. The SAS Institute Inc. Cary, NC.

Southern Pine Inspection Bureau – SPIB. 2021. Standard Grading Rules for Southern Pine Lumber, Southern Pine Inspection Bureau. Pensacola, FL.

Townsend T, Dubey B, Tolaymat T, and Solo-Gabriele H. 2005. Preservative Leaching from Weathered CCA-Treated Wood. Journal of Environmental Management 75(2):105-113.

Wang J, Wei P, Gao Z., and Dai C. 2018. The Evaluation of Panel Bond Quality and Durability of Hem-Fir Cross-Laminated Timber (CLT). European Journal of Wood and Wood Products 76:833-841.

CHAPTER IV

STRENGTH AND STIFFNESS OF 3-PLY INDUSTRIAL BAMBOO MATTING

Shmulsky, R.; Correa, L.M.S., and Quin, F. 2021. Strength and Stiffness of 3-ply Industrial Bamboo Matting. Bioresources 16(3):6392-6400. https://doi.org/10.15376/biores.16.3.6392-6400. (Republished with permission)

4.1 Abstract

There is a pressing need to develop engineering standards for timber-and other wood-based mats suitable for supporting construction vehicles, etc. In 2018, a group of mat producers and users began discussing a potential grading standard specific to mats. There are large gaps in the literature regarding the performance of the available raw materials as well as bolt-laminated mat systems. This study addresses the issue of determining the strength and stiffness values of a commercially sourced industrial bamboo mat. A total of seven 8 ft x 14 ft (2.44 m x 4.27 m) commercial bamboo mats were cut into 28 billets that were 21.5 in (54.6 cm) in width. The bamboo mat billets were evaluated for bending stiffness (modulus of elasticity [MOE]) and strength (modulus of rupture [MOR]) using a three-point static bending test. The 5th percentile non-parametric tolerance limit (5% NTL) and design value for fiber stress in bending (F_b) were calculated. The mechanical property values measured for the 3-ply bamboo mat were at least 25% less than values reported for mixed hardwood timber mats. This type of structural performance information is helpful and useful in the development of matting standards, as it describes the minimum performance characteristics for this type of composite matting.

4.2 Introduction

The development and use of industrial matting are well documented. Mats provide safe, stable, and flat work surfaces on which people, equipment, and machinery can operate during construction. In addition to providing site access for construction, they protect life, property, equipment, structures, and the environment. Mats are generally panelized. That is, their respective widths and lengths are many times greater than their thicknesses. Wood and timber are likely the most recognizable and routine materials that are used in this regard. The research related to the mechanical properties of industrial mats is gaining more attention. In particular, allowable design bending strength (F_b) based on modulus of rupture (MOR) as well as stiffness, reported as modulus of elasticity (MOE), are the two most routinely reported and used mechanical properties. Design strength allows a specifier to employ a mat under given loads and soil conditions in a safe manner with minimal risk of breakage or damage. The MOE relates to stiffness and can be used to calculate mat deflection under varying loading and soil conditions. This factor is critical with respect to overhead lifting and keeping machinery such as cranes from tipping. Ground disturbances, for example rutting, soil shear, and soil compaction are also influenced by mat stiffness. Thus, these mechanical properties influence safety, environmental protection, as well as utility value and overall costs.

Wood and timbers are likely the most recognizable materials that are used in mat construction. Past research has examined the mechanical performance of sawn hardwood timber mats (Owens *et al.* 2020). Yang *et al.* (2015) studied face-laminated low-grade hardwood lumber for use in bolt-laminated mats. Other works have investigated the composite effect of bolt laminated billets used in mats (Shmulsky *et al.* 2008) and the use of instrumentation to characterize stresses and deflection in mats during testing (Stroble *et al.* 2012). Additional timber

and mat research and information can be found in Herberg (2018), NeLMA (2017), and the National Design Specifications for wood (NDS 2018). Additional work has been reported by Xiao et al. (2021) and Li et al. (2021) on the performance of bamboo cross-laminated timber. Both of these two investigations deal with adhesive bonded bamboo. None of these, however, mention or deal with mechanical properties of bolt laminated bamboo mats. Novel materials and mat architectures are continually being developed for commercial applications. Alternatives, such as composites (including bamboo), other bio-based materials, polymers, and metals, are continually coming to market.

4.3 Materials and Methods

In this research, commercially sourced 3-ply bolt-laminated bamboo mats were evaluated. The bamboo mats were acquired through a national industrial supplier in the USA. These are available throughout North America. The raw material bamboo was grown in Asia, and the mats were manufactured in Asia prior to being imported into North America. As sourced, the mats are available in 8 ft × 14 ft (2.44 m × 4.27 m) sizes. For testing, billets of size approximately 21.5 in (54.6 cm) wide were ripped from these mats (Figure 4.1). Four billets were produced from each parent mat. Each 3-ply mat was approximately 2.63 in (6.68 cm) thick, while each single layer was approximately 0.875 in (2.22 cm) thick. Individual layers were made of crushed bamboo that had been processed into adhesively bonded panels, somewhat analogous to plywood or oriented strandboard panels. The crushed bamboo used as raw material is often referred to as scrim. The panels were manufactured with waterproof structural adhesive for intended use in industrial, outdoor, and matting applications. With respect to mat architecture, the bottom (tension) face panel consisted of bamboo fibers all oriented parallel with the long axis of the mat. The middle lamina panels consisted of the bamboo fibers running perpendicular to

the long axis of the mat. The top face (compression) panels consisted of three-layer architecture (most similar to plywood). In those top layers, the outer layer (faces) of bamboo fiber was oriented parallel with the long axis of the mat while the bamboo fibers in the middle layer of that panel were oriented perpendicular to the long axis of the mat. A schematic of this mat architecture is shown in Figure 4.2. While this mat architecture is not symmetric through the thickness, it provides a relatively balanced overall panel construction and likely develops better wear characteristics on the surface ply as compared to a uni-directionally laminated facial panel.

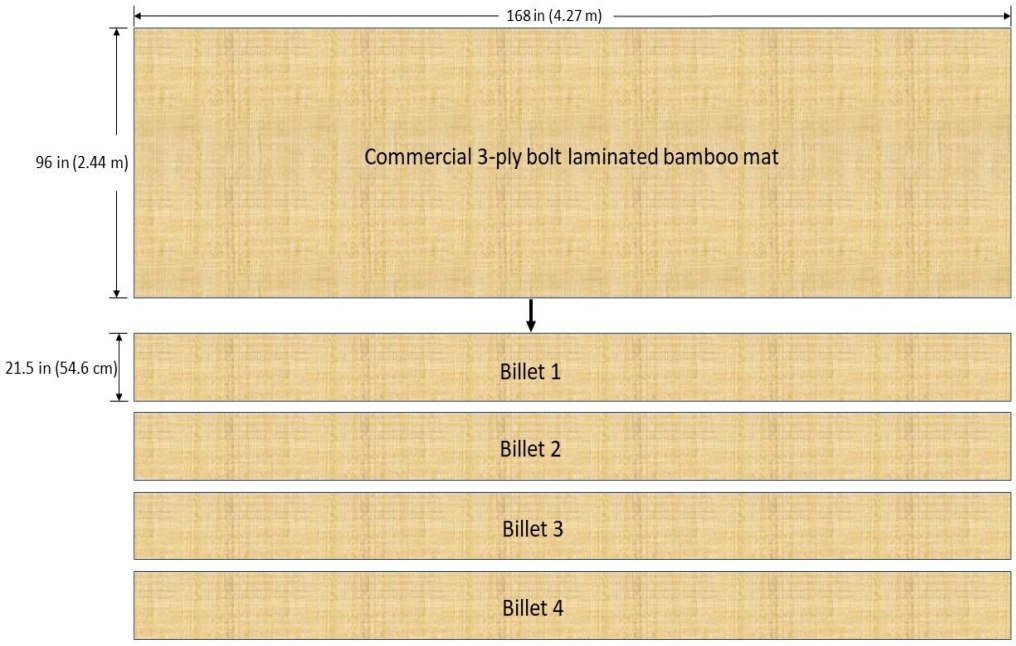

Figure 4.1 Four testing billets were cut from each 3-ply bolt laminated bamboo mat

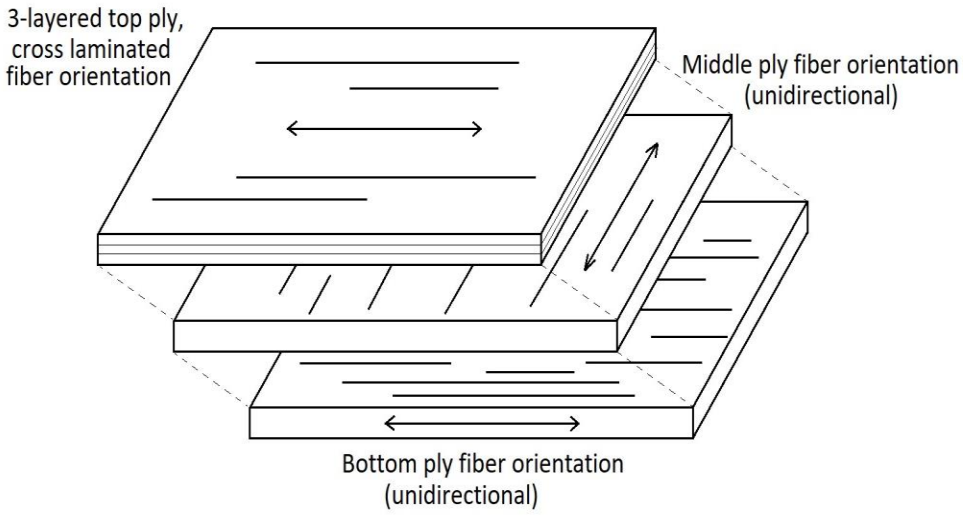

Figure 4.2 Schematic of 3-ply bolt laminated mat illustrating the fiber orientation in the bottom, middle, and top plies

Commercial bolts of 3/8-in (0.95 cm) diameter were used to fasten the plies together (bolt laminated). The bolts were installed at an approximate schedule of 1.28 bolts per square foot (13.8 bolts/m^2) of mat surface area. On the top surface, the bolt heads were set directly into the mat surface. On the bottom surface was a force distributing washer, approximately 2.5 in (6.35 cm) in diameter, was also installed between the nut and the bamboo surface

To develop a non-parametric design for bending strength value, 28 billets were tested. The billets were tested in third point bending following ASTM 5456-17 (2017) with a modified span:depth ratio. The span to depth ratio was extended, as per the guidance of APA PRG 320 (2018) to encourage bending failure and discourage rolling shear failure in the composite section for this cross-laminated composite. A 28:1 span to depth ratio was used for testing. As such, the clear span was 73.5 in (187 cm) and the load heads were 24.5 in (62.2 cm) apart (Figure 4.3). The billets were supported fully across their widths and the loads were applied across the full billet widths. The ends of the mats contained varying tongues and grooves/notches to facilitate interlocking among mats. In many cases, these tongues and grooves/notches were machined off

the specimens during preparation. In cases where their remnants remained, any remnant tongues and grooves/notches were not included in the test span. In this manner, they did not influence the strength or more importantly the deflection and resultant stiffness. A partial stack of machined billets staged for testing is shown in Figure 4.4. An exemplar photograph of a single billet in the universal test machine frame is shown in Figure 4.5.

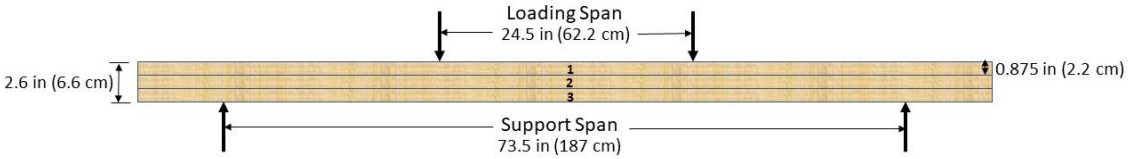

Figure 4.3 Third point loading configuration for 3-ply bolt laminated bamboo mat

Figure 4.4 Stack of machined 3-ply bamboo billets staged for mechanical testing

Figure 4.5 Exemplar picture of one billet during destructive flexural testing

With respect to section properties, the gross thickness (2.625 in) was used in calculation of section modulus and moment of inertia. When it comes to bending strength analysis, the order statistic for the 5% tolerance limit was determined per ASTM D2915-17 (2017). As such, the non-parametric 5^{th} percentile is taken as the lowest observation among a minimum of 28 ranked/sorted observations. Further, the allowable design value for fiber stress in bending (F_b) was calculated by dividing the non-parametric 5^{th} percentile by a combined load duration and safety factor of 2.1, following ASTM 5456-17 (2017). The load duration component of this factor is based on 10 years (cumulative) at full design load. The F_b calculation did not consider any adjustments to uniform loading conditions. Given that an industrial mat routinely only lasts 3 to 5 years, this number is thus considered as conservative. With respect to stiffness, the numerical average MOE is reported for design.

4.4 Results and Discussion

The performance of the tested 3-ply bamboo mats is shown in Table 4.1. The design value for F_b was 1,174 psi (8,090 kPa), and the average MOE was 279,000 psi (1,920 MPa). An exemplar load-deflection curve from one specimen is shown in Figure 4.6. This study presents a portion of ongoing testing and assessment in support of the industrial mat sector. The bolt lamination schema associated with these mats did not facilitate the development of full composite action among the plies. Therefore, bolts placement did not prevent layers from acting independently. As a result, shear between layers was greater than expected generating non-recoverable fiber crushing around bolt areas and panel's delamination (Figure 4.7). While this bolt lamination scheme may facilitate rapid production, sufficient strength, and stiffness for shipping and handling in service, it does not appear to capitalize on the full potential mechanical value, particularly with respect to MOE, of the constituent plies. For comparison, the allowable design strength (F_b) of these 3-ply bamboo mats (8,090 kPa) is approximately half of that for mixed hardwood timber mats (15,990 kPa) as reported by Owens *et al.* (2020). By similar comparison, the stiffness (MOE) of these 3-ply bamboo mats (1,920 MPa) is approximately one quarter of that for mixed hardwood timber mats (7,650 MPa) as reported (Owens *et al.* 2020). The stiffness would increase with minimal additional cost if the discrete bamboo lamina could be more securely fastened to each other and thereby develop better composite action.

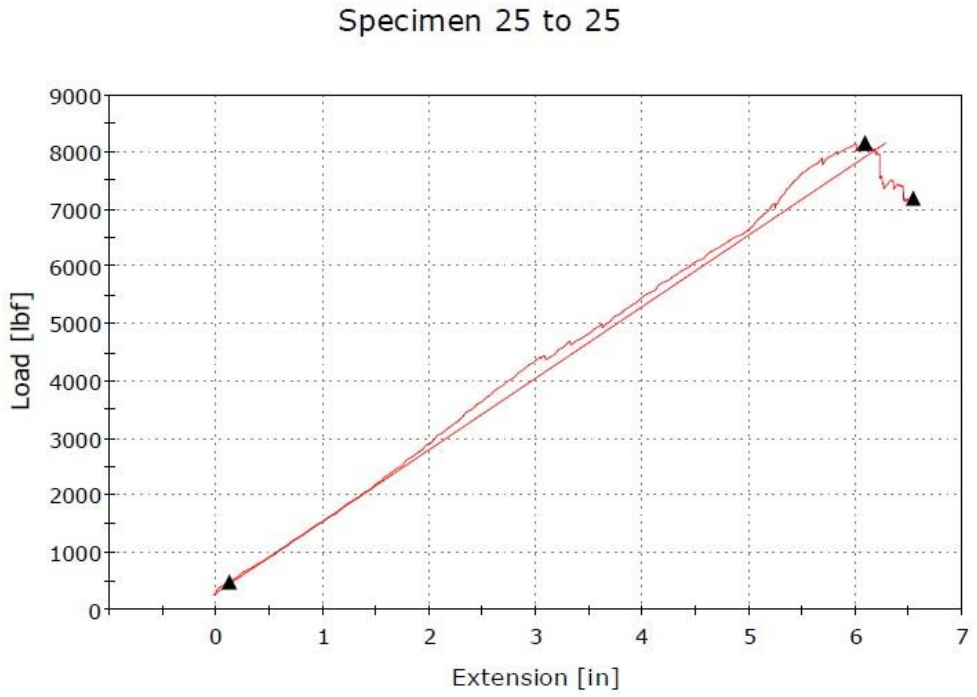

Figure 4.6 Exemplar chart of the load deflection curve of a single specimen

Table 4.1 Mechanical strength and stiffness summary statistics for 3-ply bamboo mats

	Strength (MOR)	Stiffness (MOE)
Number	28	28
Average	3,749 psi (25,800 kPa)	279,000 psi (1,920 MPa)
Maximum	5,310 psi (36,600 kPa)	320,000 psi (2,210 MPa)
Minimum	2,465 psi (17,000 kPa)	240,000 psi (1,650 MPa)
Coefficient of Variation	15.7%	6.9%
5% Tolerance Limit (95% Content, 75% Confidence)	2,465 psi (17,000 kPa)	Not applicable
F_b	1,174 psi (8,090 kPa)	Not applicable

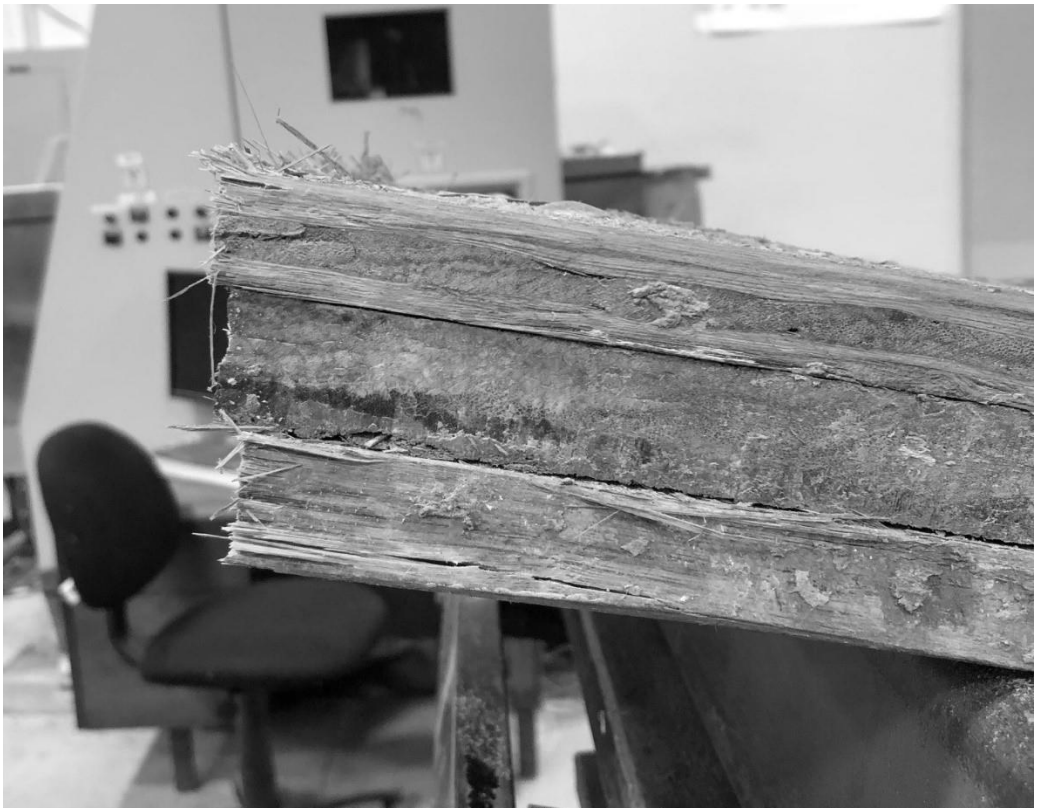

Figure 4.7 The end of an exemplar billet during mechanical testing; the sliding action of the three individual plies under flexural strain is visible

4.5 Conclusions

1. Allowable design values for flexural strength and stiffness for a commercially available bamboo mat were developed.
2. The bamboo mats performed with a relatively small coefficient of variation, particularly with respect to stiffness. This high degree of uniformity is helpful and favorable when considering structural applications.
3. The strength and stiffness values for the bamboo mats were approximately 50% and 25% less, respectively, compared to mixed hardwood mats.
4. The stiffness of the bamboo mats could be increased at a minimal cost if the bamboo layers could be more securely fastened together to behave as a single layer. Better composite action could be developed between the 3-bamboo layers, such that they acted as a single member rather than as three separate layers, much greater stiffness would be developed at that time.
5. Quantitative mechanical property information (*e.g*. MOR, Fb, and MOE) from commercially available matting materials such as this is highly valuable toward the development of matting performance standards.

4.6 Acknowledgments

This publication is a contribution of the Forest and Wildlife Research Center at Mississippi State University. This study is supported by the National Institute of Food and Agriculture, U.S. Department of Agriculture, and McIntire-Stennis Project under accession number MISZ-065940.

4.7 References

APA PRG 320 (2018). "Standard for Performance-Rated Cross-Laminated Timber," The Engineered Wood Association, Tacoma, WA, USA.

ASTM D2915-17 (2017). "Standard Practice for Sampling and Data-Analysis for Structural Wood and Wood-Based Products," ASTM International, West Conshohocken, PA, USA.

ASTM D5456-17 (2017). "Standard Specification for Evaluation of Structural Composite Lumber Products," ASTM International, West Conshohocken, PA, USA.

Herberg, E. (2018). *Flexural Performance of Nail-Laminated Timber Crane Mats*, Master's Thesis, University of Minnesota, University Digital Conservancy, Minneapolis, MN, USA.

Li, H., Wang, B. J., Want, L., Wei, P., Wei, Y., and Wang, P. (2021). "Characterizing Engineering Performance of Bamboo-Wood Composite Cross Laminated Timber made from Bamboo Mat-Curtain Panel and Hem-Fir Lumber," *Composite Structures* 266, article no. 113785, 13 pp.

NDS. (2018). "National Design Specification for Wood Construction," American Wood Council. Washington, DC.

NELMA. (2017). "Standard Grading Rules for Northeastern Lumber," Northeastern Lumber Manufacturers Association. Cumberland, ME.

Owens, F. C., Seale, R. D., and Shmulsky, R. (2020). "Strength and Stiffness of 8-inch Deep Mixed Hardwood Composite Timber Mats," *BioResources* 15(2), 2495-2500. DOI: 10.15376/biores.15.2.2495-2500

Shmulsky, R., Saucier, C. L., and Howard, I. L. (2008). "Composite Effect of Bolt-Laminated Sweetgum and Mixed Hardwood Billets," *Journal of Bridge Engineering* 13(5), 547-549. DOI: 10.1061/(ASCE)1084-0702(2008)13:5(547)

Shmulsky, R., and Shi, S. (2008). "Development of Novel Industrial Laminated Planks from Sweetgum Lumber," *Journal of Bridge Engineering* 13(1), 64-66. DOI: 10.1061/(ASCE)1084-0702(2008)13:1(64)

Stroble, M. F., Howard, I. L., and Shmulsky, R. (2012). "Wood Construction Platform Design using Instrumentation," *Wood Material Science and Engineering* 7(1), 13-24. DOI: 10.1080/17480272.2011.637132.

Xiao, Y., Cai, H., and Dong, S. Y. (2021). "A Pilot Study on Cross-Laminated Bamboo and Timber Beams," *Journal Structural Engineering*. (ASCE). 147(4), article no. 06021002, 7 pp.

CHAPTER V

CONCLUSION

This study presented three applications of expanding the market for biomaterials (wood and bamboo). The wood products industry is a major industry globally and in the United States. This study explored the structural behavior of two bolt connections presently used in the stairway industry. This will allow stair builders and designers a better understanding of how these connectors work under various loading conditions. This study only explored the use of only one hardwood species. Expanding on this study by including other hardwood species and some softwood species could be beneficial to the stairway industry.

The second part of this study explored the feasibility of post treating SYP CLT in a pressurized treating cylinder. The study proved successful in post treating CLT, and more studies need to be conducted to address the drying cycles after treating on the influence on the bonding conditions. Preliminary results of kiln drying showed that even a conservative drying cycle was not sufficient in preventing degrading of the CLT panel after post treating. The panels treated with the CA-C preservative showed a higher average BSS and a smaller delamination rate than the MCA preservative treated panels.

The last part of this study dealt with developing design values for a commercially sourced industrial grade bamboo mat. Allowable design bending strength (F_b) values along with bending stiffness (modulus of elasticity [MOE]) and strength (modulus of rupture [MOR]) were obtained

for a commercially available industrial grade bamboo mat. This information is beneficial when developing performance standards for this type of matting configuration.